Democratic and Popular Republic of Algeria
Ministry of Higher Education and Scientific Research
Faculty of Science
biology department

Assessment of bacterial cellulose biosynthesis from olive bagasse using photostimulation

Halima Khelifa

Dissertation submited to Escola Superior Agrária de Bragança to obtain the Degree of Master in Biotechnological Engineering under the scope of the double diploma with University Moulay Tahar of Saida

Supervised by

Pedro Crugeira
Paula Cristina Azevedo Rodrigues
Halla Noureddine

jury members
Mokhtar Benreguieg
Taha Ahmed Benabbou

Bragança
2024

CONTENTS

LIST OF TABLES

LIST OF FIGURES

LIST OF ABBREVIATIONS

AAB: Acetic acid bacteria

ATCC: American type culture collection

ATP: Adenosine triphosphate

BC: Bacterial cellulose

Cel-: Cellulose-deficient mutants

DNA: Deoxyribonucleic acid

DO: Dissolved oxygen

DSM: Deutsche Sammlung von Mikroorganismen und Zellkulturen

DOR: Dry olive mill residue

DTG: derivative thermogravimetric

EPS: Exopolysaccharides

FTIR: Fourier transform infrared spectroscopy

HPLC: High-performance liquid chromatography

HS: Hestrin Schramm

LED: Light-emitting diode

LMG: Laboratory for Microbiology Ghent

MCC: microcrystalline cellulose

MH: Mueller-Hinton

MOP: Moist olive pomace

NaOH: Sodium hydroxide

NBRC: NITE biological resource center

NCBI: The National Center for Biotechnology Information

OP: Olive pomace

pH: Potential of hydrogen

PCW: Primary cell walls

ROS: Reactive oxygen species

TAE: Tris-Acetate-EDTA buffer

TGA: Thermogravimetric Analysis

ACKNOWLEDGMENTS

First and foremost, I would like to express my deepest gratitude to my supervisors for their guidance and support, though words seem insufficient to convey my appreciation.

Professor Paula Rodrigues, thank you for consistently driving me forward in my work with your enthusiastic and energetic demeanor. Despite your busy schedule, you have guided me with immense kindness, perseverance, and patience. You granted me the freedom to explore my topic of interest.

I am immensely indebted to Professor Pedro Crugeira for his invaluable insights and constructive criticism at crucial moments. His timely guidance steered my work in the right direction, and he generously provided all the necessary facilities and space in the lab for conducting my experiments.

Professor Halla Noureddine has been a constant source of inspiration throughout my work. His encouragement motivates me to confront any difficult situations and challenges that lie ahead.

Thanks to my home university, for the opportunity to pursue master studies and gain valuable skills and experience in Portugal.

My sincere gratitude to engineer Jorge Sá Morais for all the help in HPLC analysis and Paula Vanessa for all the advice and guidance she gave me while working in the laboratory.

To my friend Souha for her support and wonderful time together.

To my parents, sisters, and brother, for all the love, support, and encouragement for all my pursuits.

ABSTRACT

The biosynthesis of bacterial cellulose (BC) is an innovative approach with a variety of applications. Strategies have been studied to economically enable the process, with the most common being research on fermentation media to overcome limitations and increase competitiveness in the market, thus allowing greater diversity in the use of this biopolymer. Moist olive pomace (MOP) is a byproduct of the olive oil industry that can be phytotoxic to soil and water bodies, potentially causing environmental impact. This study aimed to evaluate BC production with various concentrations of MOP (1%, 5%, 10%, 20%, 30%, and 40%) and analyze the effect of LED irradiation at 630 ± 10 nm, depositing an energy density of 14 J/cm². *Komagataeibacter intermedius* SB14, a cellulose-producing strain, was identified and studied for BC production. The characterization of cellulose membranes was performed using Fourier-transform infrared spectroscopy (FTIR), thermogravimetric analysis, mechanical testing, and evaluation of antioxidant and antimicrobial activity. A significant increase ($p < 0.0001$) in BC production was observed in the 20% MOP group, with a 166.95% increase compared to the control (0% MOP). The result indicated a cellular response due to stress caused by the phenolic compounds present, leading to increased BC production. LED light emission led to a significant increase in BC production, with 124% in the control group and 392% in the 20% MOP group. Characteristic cellulose groups were identified in all produced samples. Mechanical testing revealed greater tensile strength and deformation capacity of the cellulose membrane produced with 20% MOP (60.73 MPa and 0.696 mm/mm) compared to the control (12.75 MPa and 0.098 mm/mm), respectively. Although increased antioxidant activity was observed in the MOP-containing medium, no antimicrobial activity was detected in any of the produced samples. This work highlights a sustainable pathway by introducing MOP into the circular economy chain and leveraging LED irradiation in the bioprocess to enhance production and reduce costs.

Keywords: biopolymer; *Komagataeibacter intermedius*; moist olive pomace; LED irradiation.

RESUMO

A biossíntese de celulose bacteriana (CB) é uma abordagem inovadora com uma diversidade de aplicações. Estratégias têm sido estudadas de forma a viabilizar economicamente o processo, sendo a mais comum a pesquisa de meios de fermentação para superar as limitações e aumentar a competitividade no mercado, possibilitando assim uma maior diversidade na utilização deste biopolímero. O bagaço húmido de azeitona (MOP) é um subproduto da indústria de azeite que pode ser fitotóxico para o solo e corpos hídricos, podendo causar impacto ambiental. Pretendeu-se com este estudo avaliar a produção de CB com várias concentrações de MOP (1%, 5%, 10%, 20%, 30% e 40%) e analisar o efeito da emissão de irradiação LED em 630 ± 10 nm, depositando uma densidade de energia de 14 J/cm^2. A estirpe *Komagataeibacter intermedius* SB14, produtora de celulose, foi estudada para a produção de CB. A caracterização das membranas de celulose foi realizada por espectroscopia no infravermelho por transformada de Fourier (FTIR), análise de termogravimetria, ensaio mecânico e avaliada a atividade antioxidante e antimicrobiana.

Constatou-se um aumento significativo ($p < 0,0001$) da produção de CB no grupo 20% MOP de 166,95% em comparação com o controlo (0% MOP). O resultado indicou uma resposta celular pelo estresse causado pelos compostos fenólicos presentes e consequente aumentou da biossíntese de CB. A fotoestimulação com luz LED conduziu a um aumento significativo na produção de CB, verificando-se 124% no grupo controlo e 392% no grupo 20% MOP. Os grupos característicos da celulose foram identificados em todas as amostras produzidas. O teste mecânico revelou uma maior resistência à tração e capacidade de deformação da membrana de celulose produzida com 20% MOP, 60,73 MPa e 0,696 mm/mm, em comparação com 12,75 MPa e 0,098 mm/mm do controlo, respetivamente. Também foi constatado um aumento da atividade antioxidante com a produção em meio contendo MOP, mas não se verificou atividade antimicrobiana em nenhuma amostra produzida. Este trabalho revelou uma via sustentável com a introdução do MOP na cadeia de economia circular e de inovação tecnológica com a aplicação da irradiação LED no bioprocesso, aumentando a produção e consequente diminuição de custos.

Palavras-chave: Celulose Bacteriana; biopolímero; *Komagataeibacter intermedius*; bagaço de azeitona húmido; Irradiação LED.

1. INTRODUCTION

1.1 Framework

The last few decades have seen the development of novel, multifunctional, and biomimetic biomaterials (natural, modified natural, or synthetic) with improved properties and applications that can be used in a variety of fields, including bioprinting, regenerative medicine, and the food industry (Popa et al., 2022). Conventional materials can be successfully replaced with these biomaterials. The term "biomaterial" describes an environmentally and biocompatible beneficial substance derived from renewable resources, such as fossil fuels, agricultural raw materials, and electronic reserves (Popa et al., 2022). Among these newly tailored biomaterials, a central place is occupied by bacterial cellulose (BC), an ecological polysaccharide broadly studied for multiple applications due to its excellent physicochemical and biological properties (Matsumura & Rajan, 2021). It has been used to make a variety of products, including desserts with a high dietary fiber content, artificial skin for medical treatments, acoustic diaphragms, artificial blood vessels, and electric conductors, it has also been incorporated as a food stabilizer and used for the reinforcement of other polymeric materials or paper (Velásquez-Riaño, 2017).

Several bacteria can synthesize cellulose, including the genera *Acetobacter*, *Gluconobacter*, *Komagataeibacter*, *Rhizobium*, *Agrobacterium,* and *Sarcina*. *Komagataeibacter intermedius* is a Gram-negative rod-shaped species commonly found in fruit juice, wine vinegar, and Kombucha (Devanthi et al., 2021). It can make BC in various pH conditions (4–9 pH), and it can produce the most BC in a short time when the environment is more basic at 30 °C (Devanthi et al., 2021). However, the optimal conditions depend on the specific requirements of the bacterial strain (Przygrodzka et al., 2022).

The yield and properties of BC depend on several factors, including the bacterial strain used, the culture medium composition, and the operational conditions applied during the cultivation process. The major challenges faced for the applications of BC and its up-scale production are the high cost of the media and low productivity at the industrial scale. Currently, the possibility of solving this issue is combined with using by-products and waste from the food industry and agricultural production as feedstocks to prepare cultivation media. Utilizing renewable carbon sources through bioprocess optimization is a feasible way to escape the current scenario while reducing the need for pricey commercial media and low productivity. Using industrial residues or wastes containing sugars can lower the cost of nutrients to nearly zero while simultaneously supporting the goals of the circular economy (Campano et al., 2016).

In the Mediterranean area, where olive cultivation is widespread and the volume of effluents produced is great, treatment and disposal of residues from olive oil processing represent

one of the main problems faced by industries involved in the extraction of olive oil. Portugal is the fourth most powerful country in the world in the olive oil sector, with 52% of its cropland (366 000 ha) comprising olive tree culture (Almeida et al., 2019). Wastewater, especially the wash water of the process, and bagasse, a solid waste with pulp, pits, husk, and some oil and water, are the main by-products of the olive oil industry (Almeida et al., 2022). Recently, some studies have dealt with olive residues on energy generation and activated carbon production. For example, a source of sugar-rich aqueous extracts from the residue of dry olive mills has been used to produce BC (Ahmed & Hassan, 2023).

Low-power light-emitting diodes (LED) irradiation, emitting in certain parameters (wavelength, power, energy density, and irradiated surface), has been shown to be biostimulatory (Passarella & Karu, 2014). One of the biological targets of irradiation in the red spectrum are terminal enzymes of the respiratory chain such as cytochrome c oxidase, increasing the rate of electron flow and consequently increasing the amount of cellular ATP available. Photoexcitation induces allosteric changes in cytochrome c oxidase and/or in flavin components of the chain, such as NADH dehydrogenase, which can cause other redox changes and modulate biochemical reactions through a chain of transduction and amplification of the light signal towards biological macro-effects, such as increased cell proliferation via increased DNA synthesis (Crugeira et al., 2018; Karu et al., 2004). Radiation emission can also activate intracellular metalloproteins that actively participate in the biosynthetic pathway of BC production. Photon absorption by prosthetic groups can increase anabolic capacity or help maintain the three-dimensional conformation of enzymes, making them more resistant to denaturation promoted by metabolic action (Kopka et al., 2017).

1.2 Objectives

The objective of this work is to develop and optimize a high-yield, low-cost bioprocess to produce BC from a previously isolated strain of *K. intermedius* using agricultural waste (moist olive pomace) and LED irradiation.

The specific objectives are:

1. To assess the production of BC by a strain of *K. intermedius* under static conditions.
2. To assess and optimize the BC production ability of the *K. intermedius* strain and the BC properties using moist olive pomace as substrate.
3. To evaluate the effect of LED irradiation (ʎ630 nm) on the yield and properties of BC.
4. To characterize the BC produced under the established conditions.

2. LITERATURE REVIEW

2.1 Cellulose – general aspects

Cellulose is regarded as the most abundant biopolymer in nature. Payen (1838) was the first to discover this substance, he isolated it and defined its chemical structure (Krzysztof Jadczak, 2023). Cellulose is a linear homopolysaccharide polymer of β-D-glucopyranose units covalently linked together by β-glycosidic bonds (Liang, 2023), whose chemical formula is $(C_6H_{10}O_5)n$ (the n of the degree of polymerization), as shown in Figure 1 (Klemm et al., 2005). Each link consists of the hydroxyl group of one glucose and the protentional aldehyde group of another. Three hydroxyl groups make up each glucose monomer of cellulose; the primary hydroxyl groups are located at C6, while the secondary hydroxyl groups, which can generate intra and intermolecular hydrogen bonds, are located at C2 and C3. Consequently, because of its chemical makeup and spatial conformation, cellulose frequently exhibits a highly organized structure (Urbina et al., 2021).

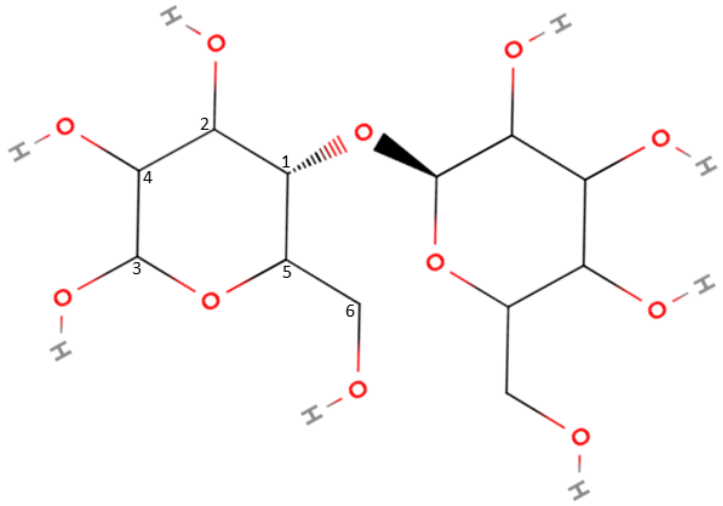

Figure 1. Molecular structure of cellulose (Klemm et al., 2005).

The main source of this material is the plant cell wall (Almeida et al., 2022). The cellulose molecules that are arranged in the cell walls into microfibrils have characteristic orientations, or helix angles, that vary depending on the layer of the cell wall and the

species of plant (Klemm et al., 2005). Their existence plays a key role in determining the characteristics of the plant cells, particularly their durability and mechanical qualities. Even while cellulose makes up 40–50% of the mass of the cellular walls, other substances are also present, including pectin (35%), hemicellulose (30%), and lignin (9–18%) (Krzysztof Jadczak, 2023).

Commercial cellulose production concentrates on harvested sources such as wood or naturally highly pure sources such as cotton. The finest type of cellulose found in nature is found in the seed hair of Gossypium plants, or cotton (Dochia et al., 2012). Fiber primary cell walls (PCW) are composed of structural wall proteins and carbohydrate polymers such as cellulose, hemicellulose, and pectin. The expanding PCW has less than 15% of its weight in cellulose, while mature fibers have a thicker secondary cell wall made up of almost 95% cellulose (Fang, 2018) as shown in Figure 2 (Dochia et al., 2012). Cellulose from different sources has different properties.

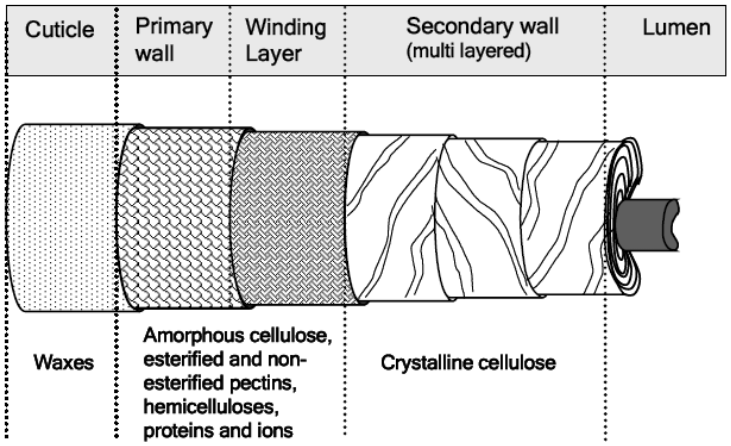

Figure 2. A schematic representation of mature cotton fiber showing its various layers (Dochia et al., 2012).

Other than plants, cellulose is also produced by some bacteria, algae, and fungi (Klemm et al., 2005). As for bacteria, mostly gram-negative strains such as *Acetobacter, Agrobacterium, Escherichia, Enterobacter*, *Gluconoacetobacter* (formerly Acetobacter), *Komagataeibacter* (formerly *Gluconoacetobacter)*, *Pseudomonas, Rhizobium, Salmonella* and *Sarcina* are some of the bacterial genera reported to produce cellulose as an extracellular film (Klemm et al., 2005). Such a type of cellulose is called microbial cellulose or bacterial cellulose (when bacteria is the source of origin). The cellulose synthesized by the bacteria aids in adhesion and aggregate to a substratum (biofilm

formation), protection of bacterial cells from harmful UV radiation, resistance to adverse environmental conditions, quorum sensing, and provides an aerobic environment for the bacteria (Augimeri & Strap, 2015).

2.2 Bacterial cellulose

2.2.1 Structure

Bacterial cellulose ($C_6H_{10}O_5$) is composed of an assembly of glucan chains (Mensah et al., 2022). The chains consist of linear glucopyranose rings, connected by β-D-1 and 4 linkages (between the OH located between C1 and C4 carbons). The number of glucose molecules also ascertains the degree of polymerisation (DP) of the cellulose polymer. This number can vary depending on the source of their origin or the synthesis conditions in the lab (Brown, 1996). It comprises a three-dimensional fibrous network of nanofibers arranged to form a hydrogel sheet, with sizes ranging from 50 to 80 nm in width and 3 to 8 nm in thickness (Khan & Kamal, 2021).

2.2.2. What makes bacterial cellulose unique?

Compared to plant cellulose, which comprises hemicellulose, lignin, and pectin, BC possesses inherent physical and mechanical properties (Figure 3) superior to plant cellulose (PC). It is pure, with a degree of polymerization between 4000 and 10,000 anhydroglucose units. In addition, it has better mechanical strength (100–160 GPa for a single fiber, like steel or Kevlar, higher crystallinity (80–90%), high water holding capacity (up to 100 times its own weight), moldability, and thermochemical stability (Hussain et al., 2019). Furthermore, in its first chains, BC generates lengthy nanofibrils that measure around 1.5 nm. The surface area of BC nanofibrils is larger than that of plant cellulose fibrils. Additionally, BC contains subfibrils that crystallize into microfibrils, forming bundles of microtapes. It is not toxic or allergic, has a lower microtape diameter, and is metabolically inactive (Reis et al., 2019). Some of the common physical properties of PC and BC are listed in Table 1 (Vadanan, 2020).

Table 1. Physical properties of plant cellulose and bacterial cellulose (Vadanan, 2020).

Properties	Plant cellulose	Bacterial cellulose
Fibre width	1.4-4 x 10-2 mm	70-80 nm
Crystallinity	56-65%	70-90%
Degree of polymerization	10000-14000	2000-8000
Young's modulus	5.5-12.6 Gpa	15-30 Gpa
Water content	60%	98.5%

Figure 3. Various properties of BC (Hussain et al., 2019).

2.2.3 Cellulose-producing bacteria

In 1886, Brown was studying *Bacterium aceti* in a nutrient culture medium that contained 1 % (w/v) acetic acid from the vinegar and red wine diluted with an equal amount of water. He observed a clear, gelatinous layer forming on top of the nutrient solution after several days of incubation. (Vadanan, 2020). Extracellular cellulose fibers are produced by bacteria under either static or dynamic circumstances, and the yields vary based on the species and substrate of the growth media.

According to recent research, a variety of bacteria, including Gram-positive and Gram-negative species including *Sarcina ventriculi*, *Rhizobium* spp., *Agrobacterium* spp., *Acetobacter* spp., *Azotobacter* spp., *Pseudomonas* spp., and *Salmonella* spp., can manufacture cellulose (Wang et al., 2019). The cellulose produced by various bacteria differs in terms of their appearance, structure, and characteristics. Table 2 lists some strains capable of producing cellulose (Wang et al., 2019).

Table 2. Different bacterial strains and the morphological nature of the cellulose (Wang et al., 2019).

Microorganisms	**Morphological nature of cellulose**
Acetobacter/ Komagataeibacter	Fibril structure/ Ribbon structure
Achromobacter	Ribbon structure
Agrobacterium	Fibril structure
Aerobacter	Fibril structure
Alcaligenes	Fibril structure
Pseudomonas	Amorphous
Rhizobium	Short fibril
Sarcina	Fibril structure

Species from the genus *Komagataeibacter* have been identified as particularly important bacteria producing BC (Hsu et al., 2022). This genus is a member of the acetic acid bacteria (AAB) group, and some of them are capable of producing two distinct types of cellulose, known as cellulose I and cellulose II, each with a unique microfibrillar structure. A polymer that resembles a ribbon, known as crystalline cellulose, makes up cellulose I, whereas an amorphous polymer makes up cellulose II (Hernández-Arriaga et al., 2019).

Komagataeibacter intermedius is a species that is frequently found in Kombucha, wine vinegar, and fruit juice (Devanthi et al., 2021). Compared to *K. xylinus*, a typical BC-producing bacteria, *K. intermedius* strain from a commercial wine vinegar had a 48% higher ability to produce BC. The produced BC was also pure, had a high crystallinity index, and had similar mechanical properties to the one made by *K. xylinus* (Devanthi et al., 2021). *Komagataeibacter intermedius* can produce BC within a wide pH range (4–9),

and maximum production can occur within a short period in alkaline conditions (Devanthi et al., 2021). It has been found to produce a higher output of BC in sugarcane molasses, a less expensive option to the commercial media currently used for BC production (Devanthi et al., 2022).

AAB oxidize the ethanol that yeasts hydrolyze and consume to produce acetic acid, and it also activate the cellulose-synthase machinery in the liquid-air interface under static conditions. It has been reported that symbiotic relations between AAB and the acid-tolerant and osmophilic yeasts enhance cellulose yield production due to synergic microbial metabolism (Jayabalan et al., 2014). Because kombucha tea fermentation is a naturally occurring symbiotic culture of bacteria and yeasts, commonly referred to as SCOBY, it presents a great chance to get bacterial cellulose by taking advantage of these symbiotic relationships among microorganisms (Jayabalan et al., 2014).

2.2.4 Bacterial cellulose biosynthesis

The synthesis of bacterial cellulose occurs when oxidative fermentation takes place in a medium that is either synthetic or non-synthetic (Popa et al., 2022). The bacterial cytoplasm is the source of bacterial cellulose, which is then produced in the microorganism's membrane (Popa et al., 2022). The biosynthesis of bacterial cellulose involves several key enzymes that control cellulose synthesis, including glucokinase, isomerase, phosphoglucomutase, UDPG-pyrophosphorylase, and cellulose synthase (Lin et al., 2013). With glucose as a substrate, glucokinase converts it to glucose-6-phosphate by adding a phosphate group as the first step (Moniri et al., 2017). The enzyme phosphoglucomutase then converts glucose 6-phosphate to glucose 1-phosphate by changing the position of the phosphate group, followed by the transition of glucose-1-phosphate to uridine diphosphate glucose (UDP-glucose) by UDP-glucose pyrophosphorylase, preceded with cellulose synthesis by UDP-glucose synthase (Naomi et al., 2020). UDPG is a direct precursor of cellulose that is found in a wide variety of species, glucosyl residues from UDP-glucose are transferred to the developing b-D-1,4-glucan chain by cellulose synthase (Moniri et al., 2017). The bacterial cellulose synthesis stage at a cellular (microscopic) level is illustrated in Figure 4.

The synthesis process in the bacteria’s cell will generate a straight glucose chain. The glucose will exit the bacteria through small pores in their wall. The glucose will join to make the

microfibrils. The cellulose ribbon will form from the buildup of these microfibrils over time (Naomi et al., 2020).

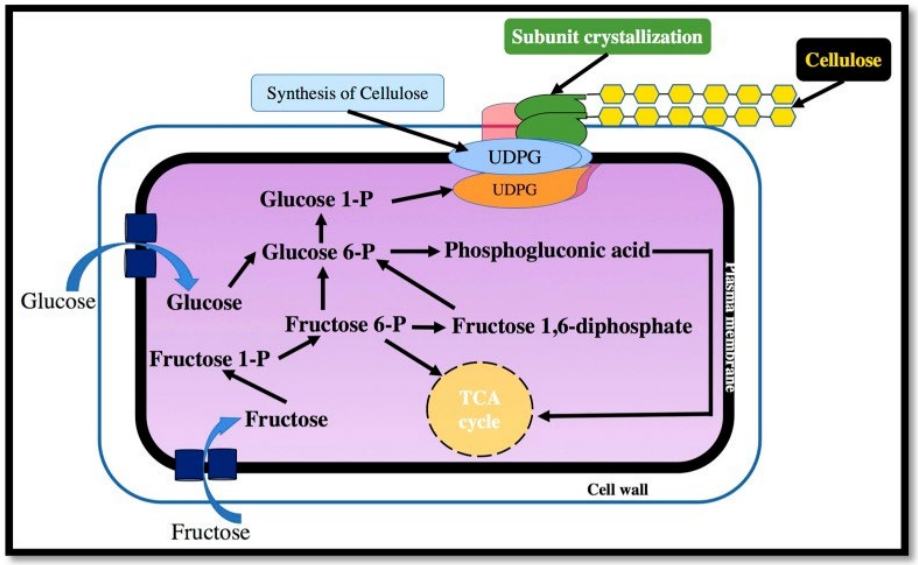

Figure 4. Biosynthetic pathway of cellulose in the cells of microorganisms (Moniri et al., 2017).

2.2.5. Bacterial cellulose production processes

Several methods have been reported to produce BC, including static culture, agitated culture, and numerous designed bioreactors, depending on the application of BC which are based on cheap approaches. To satisfy the commercial demand for BC, large-scale, semicontinuous, and continuous fermenters have been designed. The aim is to achieve maximum production of BC with suitable form and properties for the required application.

2.2.5.1.Static cultivation

The widely used static culture method, which is a conventional technique for producing BC, causes a gelatinous cellulose membrane to form on the medium's surface (Wang et al., 2019), after the medium is placed in shallow trays, inoculated, and grown for five to twenty days, or until the cellulose almost completely fills the tray (Lin et al., 2013). BC takes the shape of the container during static conditions (Raghavendran et al., 2020), retains its regular shape, and keeps its 3D interconnected reticular structure. Bacterial cellulose production under static conditions is illustrated in Figure 5 (Wang et al., 2019).

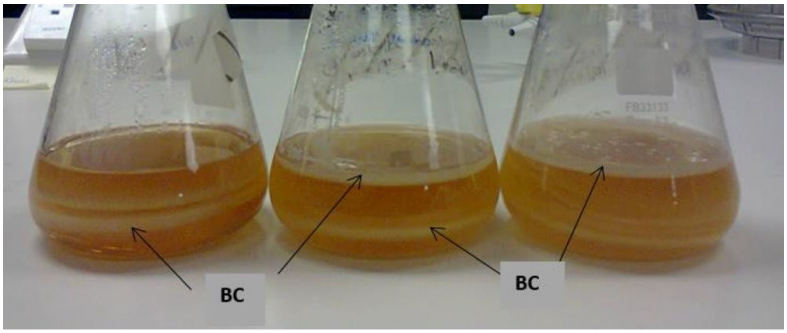

Figure 5. Preparation of BC membrane using static culture method (Wang et al., 2019).

Because pellicle production occurs at the air-liquid interface in static culture, the surface area of the culture medium has an impact on pellicle formation (Okiyama et al., 1992). The duration of the incubation period, which is typically no more than 14 days, determines the membrane's thickness because prolonged fermentation periods allow an accumulation of inhibitory metabolites such as formic and glycolic acids, among others (Urbina et al., 2021), which tends to decrease the pH of the medium. Static methods are not ideal for large-scale production due to the long production times and low productivity of thick pellicles. This threatens the economic viability of traditional static culture and hampers its industrial application. However, static fermentation of BC is more suitable for various applications due to the uniformity of the static cellulose matrix, unlike the stirred mode in which they are produced in the form of irregular spheres or pellets.

2.2.5.2.Agitated cultivation

With static culture systems, the two main issues are high cost and low production rate. It has been suggested that using an agitated/shaking culture can help resolve these issues. Asterisk-like, sphere-like, pellet-like, or irregular masses are the product of the agitated/shaking culture (Wang et al., 2019), depending on the applied rotational speed**.** BC is produced in an environment where the constant rotation of culture media and cells provides a homogenous contact resulting in better yield. When BC production happens in an agitated incubator, cellulose particles with irregular and spherical shapes are formed, unlike in static incubation. BC from agitated conditions has a lower crystallinity index,

mechanical strength, and polymerization degree than BC from static conditions (Avcioglu, 2022).

The generation of BC is impacted by the disruption of oxygen distribution in the broth caused by the increased viscosity of the culture media. The two main drawbacks of this mode of fermentation are non-uniform bacterial sizes and shapes, and inconsistency in oxygen supply, and the development of cellulose-deficient mutants (Cel-). Shear stress induced in these cultures or under these conditions causes (Cel-) to be formed, which promotes the creation of by-products that vary depending on the strain of bacteria (Campano et al., 2016).

2.2.6. Parameters controlling BC production

Several parameters such as dissolved oxygen, pH, and temperature, independent of static or agitated cultivation, need to be optimized to improve BC yield (Lee et al., 2014). Microorganisms rapidly respond to these factors in terms of induction and repression of protein synthesis and changes in cell morphology.

2.2.6.1.Temperature

Temperature is one of the most crucial factors since it affects an organism's natural homeostatic physiology, which controls how it adapts to survive. The optimal temperature of BC production by *K. xylinus* has been set to be 30 °C when cultivated for 7 days under static conditions (Lee et al., 2014; Wang et al., 2018). While the BC yield was not considerably reduced when the culture temperature was lowered from 30 °C to 25 °C, it was decreased when the temperature was raised to 35 °C (Lee et al., 2014). In BC production by *K. intermedius,* BC layer growth was observed in both single and co-culture with the yeast *Dekkera bruxellensis* during the first three days of fermentation at 30 °C (Devanthi et al., 2021).

2.2.6.2.pH

The pH is another critical parameter that influence the process of bacterial growth and fermentation, as it is an essential physiological factor that determines the physiology,

enzyme activity, and chemical environment of the bacteria. The pH is essential for both microbial growth and bacterial cellulose production, as each microbe has a specific pH range that allows growth (Bhat et al., 2012).

Komagataeibacter species are well known for their capacity to produce a variety of organic acids, including acetic acid, gluconic acid, and glucuronic acid, which lower pH levels. *Komagataeibacter intermedius* may synthesize BC in a wider pH range (4–9) than *K. xylinus*, and in alkaline conditions, maximum production can occur quickly (Devanthi et al., 2021). The pH of the fermentation medium depends on the type of carbon source used as the nutrient source (Keshk & Sameshima, 2005). Sugars such as glucose metabolise to acids, as a result, pH value drops, and BC synthesis is affected (Kongruang, 2008). Santoso et al. (2020) conducted a fermentation using *K. intermedius* FST213-1 in a Hestrin–Schramm (HS) medium with an initial pH of 8.0 and found the pH to drop to ~4.0 after 4 days, which remained constant until the end of the fermentation.

2.2.6.3.Oxygen Level

The dissolved oxygen (DO) is an important parameter to ensure proper cellular growth of the bacteria along with proper cellulose synthesis. Fernández et al. (2019) reported that the higher value of DO in the fermentation medium caused the increase in the gluconic acid, which in turn slowed down BC production. On the other hand, low DO results in a diminished growth rate of bacterial cells and BC yield. Hwang et al. (1999) determined that the highest cellulose yield was obtained in fed-batch cultures in which the dissolved oxygen concentration was controlled at 10% saturation.

2.2.6.4.Effect of carbon and nitrogen sources on BC production

The carbon source is considered one of the most important factors for effective optimization, it is used by the microorganism to convert the substrate into cellulose. The most widely used synthetic complex growth medium for BC production is the Hestrin–Schramm (HS) medium, with glucose as a carbon source for bacterial growth and BC synthesis. Yim et al. (2017) studied sucrose, corn syrup, honey, and fructose as carbon sources, and green tea, corn silk tea, rooibos tea, and black tea as nitrogen sources. Bacterial cellulose production yield was higher when green tea was used as a nitrogen

source, and among all carbon sources, sucrose presented the highest production yield. A study by Ramana et al. (2000) reported that the optimal nitrogen substrate for an organism varied according to the carbon source in the medium and between different combinations of single carbon sources and single nitrogen, *Acetobacter xylinum* (currently *K. xylinum*) preferring casein hydrolysate or peptone in the presence of sucrose or mannitol as the carbon source.

2.3 Bacterial cellulose production from various industrial wastes

2.3.1. Agro-industrial wastes

The use of industrial waste for BC production is an economically beneficial approach that helps in waste management and environmental cleaning, and reduces the cost of waste disposal for industries. Depending on the system and type of agricultural activity, these wastes have different compositions. Some are mostly made up of cellulosic compounds with fatty acids and essential oils, while others are primarily made up of lignocellulosic biomass rich in carbs, protein, and nitrogen. They are quite promising for BC production because of these features (Urbina et al., 2021).

Experimenting with different combinations of banana peel extract and glucose, Hussain et al. (2019) found that these could partially substitute conventional nitrogen and carbon sources for BC production. Kumbhar et al. (2015) used pineapple and watermelon peels for BC production, and compared the morphology of the obtained BC with the one grown in HS medium. They observed that the ribbons of the BC obtained in HS medium were longer and more uniform, and concluded that changing medium components (mixture of sugars) led to different assembling patterns. Furthermore, being a by-product of the olive oil industry, olive pomace may be an excellent option for producing reducing sugars, which would act as a source of carbon for the bacterial cellulose production process (Sagdic-Oztan et al., 2023).

2.3.2. Olive oil by-products

During olive oil processing, a variety of wastes and by-products are produced. The main ones with major nutritional and technological interest, under the scope of this review, are the olive pomace, the olive mill waste waters, the olive leaves, and the olive

stone and seed. These byproducts are thought of as low-cost raw materials that include bioactive compounds and can raise the profitability of pharmaceutical formulations, functional foods, nutritional supplements, packaging materials, and nutraceuticals (Figure 6).

Different techniques can be used to extract olive oil. The most common processes that are used are traditional pressing mills (mainly employed by small producers), the three-phase system, and the two-phase system (Abu Qdais & Al-Widyan, 2016). In the two-phase system, in which no water is added, the only produced by-products are a humid semi-solid pomace and olive oil (the product). Nevertheless, the resulting olive pomace has a high moisture content, which impairs proper storage (Abu Qdais & Al-Widyan, 2016). Despite this, olive oil producers are using this environmentally friendly two-phase method because it simultaneously reduces wastewater volume and yields a liquid/solid by-product that is high in bioactive components and leftover olive oil.

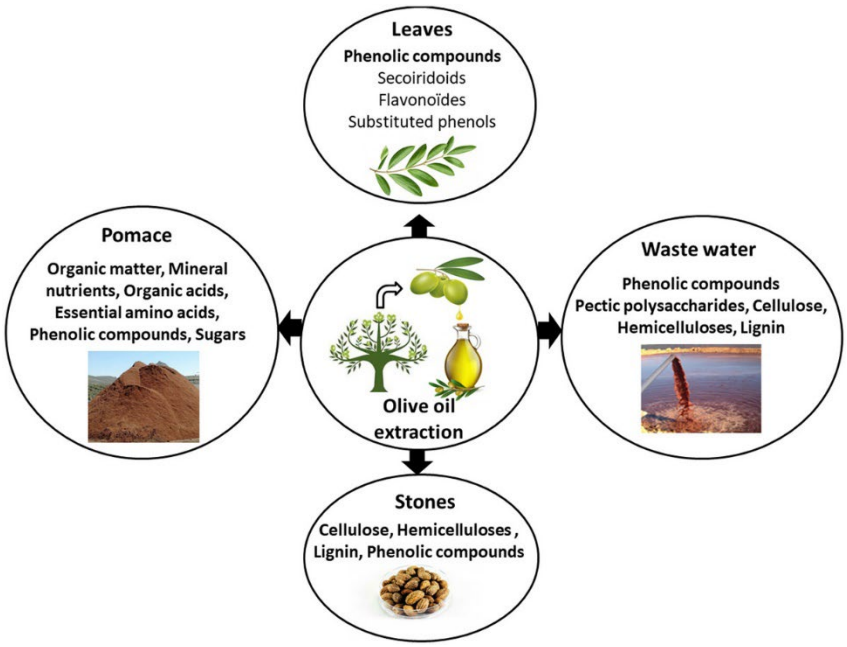

Figure 6. Main components of olive byproducts (Khwaldia et al., 2022)

2.3.3. Olive pomace

Olive moist pomace is the primary by-product of the olive industry consisting of the fruit's pulp, stones, and skin (Berbel & Posadillo, 2018). With a 15,655,000-ton yearly production capacity and characteristics including low pH, a high load of organic

pollutants, and phytotoxicity, it has become a significant environmental problem (Khwaldia et al., 2022). Although the specific characteristics of OP may differ according to the type of oil extraction, olive pomace is lignocellulosic, with cellulose, hemicellulose, and lignin making up 90% of its dry weight, along with a sizable quantity of protein (Kazan et al., 2015).

Over the last decade, olive mills have changed from a three-phase extraction technique to a two-phase extraction system. Because the two-phase system produces very little wastewater, this modification increases olive oil quality while lowering wastewater disposal expenses. However, it produces wet olive pomace or crude olive pomace (COP) (Leite et al., 2016). Two-phase olive mill waste (also known as 'olive wet husk', 'olive wet pomace', or 'olive wet cake') is a solid waste with a strong odor and a doughy texture that is difficult to manage and transport (Berbel & Posadillo, 2018).

Considering that olive pomace is composed of the remaining olive constituents, it contains a wide range of compounds that can be produced using various extraction methods. Olive pomace chemical compounds, particularly polyphenols, stand out as a potentially important by-product. Indeed, its primary functional capabilities appear to be directly related to its high phenolic content, and hence its antioxidant properties have been investigated (Nunes et al., 2016). Olive pomace is rich in hydroxytyrosol (with health benefits related to its antioxidant properties) but also has a significant content in oleuropein, tyrosol, caffeic acid, p-coumaric acid, vanillic acid, verbascoside, elenolic acid, catechol, and rutin (Nunes et al., 2016). It has been shown that dry olive mill residue (DOR), which represents 35% for the mass of the original dry OP, can be used as nutrients and carbon sources for bacterial cellulose production (Gomes et al., 2013).

2.3.4. Moist olive pomace (MOP)

The "two-phase" approach significantly lowers the amount of water required for the centrifugal extraction process, leaving only moist olive pomace (MOP), which is a mixture of olive skins, pulp, pits, and some residual oil. Moist olive pomace has a low viscosity and high moisture content, making it difficult to transport, store, and dry, which lowers its commercial worth (Crugeira et al., 2023). It contains a multitude of bioactive substances that fall into multiple categories: basic phenols (e.g., tyrosol and hydroxytyrosol) and their derivatives; derivatives of benzoic and cinnamic acid (e.g.,

gallic acid, syringic acid, caffeic acid, p-coumaric acid, verbascoside); flavonoids (e.g., apigenin, luteolin, rutin); and secoiridoids (e.g., oleuropein and oleuropein aglycone isomers (Madureira et al., 2021). Oleuropein and hydroxytyrosol are thought to be the most researched biophenols. Because of their greater and more varied health-related activities, as well as their abundance in the majority of olive byproducts (Khwaldia et al., 2022), all of the phenolic components found in olive extracts support their antioxidant activity, indicating that using the extract rather than the pure chemicals is a viable option (Contreras et al., 2020).

Olive pomace has been studied to produce BC, biogas, and antioxidants (phenolic compounds) (Sar & Yesilcimen Akbas, 2022). It has been reported that certain phenolic compounds, such as gallic acid, caffeic acid, catechol, and pyrogallol, can increase the production of BC by certain strains of *Acetobacter* spp., by acting as iron-chelating agents (Urbina et al., 2021). With the addition of phenolics, oxidation reactions involving hydroxyl radicals with cellulose dominate the minor reaction of ozone radicals with cellulose.

2.3.5. Microbial stress and cellular response

Microbial stress is a phenomenon where microorganisms respond to various environmental changes and stresses. Stressors include oxidants, nutrient deprivation, hypo/hyper-osmolarity, extreme pH, extreme temperature, and antimicrobial substances (Nizer et al., 2020). Microbes have evolved different strategies to cope with stress, such as modifying their cell structure and function, activating stress response genes and pathways, producing protective molecules, forming biofilms and aggregates, and developing resistance mechanisms (Prabhakaran et al., 2016) to enable them to survive and even thrive in many diverse and diverse environments. It can operate against bacterium cells through a variety of mechanisms, including interactions with proteins and bacterial cell walls, modifications to cytoplasmic activities and membrane permeability, suppression of energy metabolism and DNA damage, and suppression of bacterial cell synthesis of nucleic acids (Lobiuc et al., 2023).

Certain derivative compounds can also act as inhibitors of enzymes, substrates, or cofactors involved in these processes, or as chelating agents that reduce the availability of micronutrients essential for bacterial growth (Casadey et al., 2021) and can interact

with the lipid bilayer of the bacterial membrane, causing leakage of cytoplasmic contents, disruption of membrane potential, or inhibition of membrane-associated transporters and receptors (Casadey et al., 2021). Phenolic chemicals can also induce reactive oxygen species (ROS) in bacteria, such as superoxide anion, hydrogen peroxide, and hydroxyl radical, which can result in oxidative stress (Shalaby & Horwitz, 2015).

Exopolysaccharides (EPS) are complex carbohydrates that are secreted by some bacteria outside their cell membrane. They have various functions, such as protecting the bacteria from environmental stress, facilitating nutrient uptake, and forming biofilms (Dağbağlı & Göksungur, 2017). Cellulose and acetan are two types of EPS produced by *Komagataeibacter.* The biosynthesis and export of these EPS are regulated by a signaling molecule called cyclic diguanylate (c-di-GMP), which binds to specific enzymes and activates them (Poulin & Kuperman, 2021). The structure and composition of EPS produced by *Komagataeibacter* depend on several factors, such as the bacterial strain, the culture medium, the temperature, the pH, the oxygen level, and the type of induced stress.

2.4. Photobiomodulation

2.4.1. Light-emitting diode (LED)

The LED is a semiconductor that emits light in a safe manner because it is a cold lightning and has neither mercury nor glass envelopes. Moreover, one attribute of LEDs is their ability to produce various colors based on their composition, making them both energy-efficient and ecologically beneficial. Blue lights are composed of gallium, nitride, and silicon carbide, whereas red, green, yellow, and orange lights are formed of indium, gallium, aluminum, and phosphide (Finardi et al., 2021).

Several biomolecules found in mitochondria and/or other cell compartments, such as adenine nucleotides, nucleic acids, cytochrome oxidase, and some proteins, are light-sensitive and undergo significant biochemical changes (Passarella & Karu, 2014). The chromophore cytochrome c oxidase has intramolecular targets, such as copper centers, that can absorb light. This metal is present in various gram-positive and gram-negative bacterial enzymes (Crugeira et al., 2018).

According to AlGhamdi et al. (2012), photobiostimulation is mediated by the electron transport chain enzymes in mitochondria. This results in elevated rates of cell

respiration, which are then utilized by cytochrome c or the endogenous porphyrins in the cell to enhance cellular activity and metabolism. Irradiation also leads to increased ATP synthesis (Passarella & Karu, 2014). Irradiation with 663 nm light altered some NADH-linked dehydrogenase reactions where oxidation of their pools leads to changes in the redox state of mitochondria and cytoplasm (Karu, 1999).

2.4.2. Microbial photo-stimulation

Photo-stimulation is using light to artificially activate biological compounds, cells, tissues, or even whole organisms. Photo-stimulation can be used to probe various relationships between different biological processes noninvasively. It functions by stepping up energy bioprocesses linked to the accelerated biomass growth of the chosen microorganisms. This novel approach aims to maximize the phenotype without changing the genotype. Therefore, it is thought that large-scale photo-stimulation is a viable strategy for the effective and sustainable production of biomass and bioenergy (Pinheiro et al., 2020). For instance, utilizing a laser or LED to stimulate microbial cultures briefly might boost the synthesis of various bioactive compounds (Pinheiro et al., 2020).

It has been demonstrated that photo-stimulation of microorganisms to accelerate the degradation of cycle hydrocarbons works effectively in a variety of situations, including microbial consortia and isolated bacteria and fungi, and both laser and LED light irradiation caused increased cellular proliferation, protein production, and metabolic activity (Crugeira et al., 2019). It was also demonstrated that differently constituted Xanthan gum was produced by *Xanthomonas campestris* cultures that were cultivated in various culture mediums and subjected to photo-stimulation using a laser or LED (Pinheiro et al., 2020).

3. MATERIALS AND METHODS

3.1 Identification of the cellulose-producing bacterial strain

The cellulose-producing bacterial strain SB14 (= CIMO 21LE010) was previously isolated from kombucha tea, and tested in our laboratory for the production of bacterial cellulose (Leite, 2021; Petrosian, 2021). Although already identified molecularly (GenBank Accession number OK274317; Leite, 2021), the strain was submitted to a confirmation of identity, to discard contamination problems. For that, a preliminary identification was performed consisting of morphological and physiological parameters based on Gram straining using the protocol described by Moyes et al. (2009) and observation using an optical microscope (Leica DM500) coupled to a digital camera (Leica ICC50W).

The strain was then molecularly identified by amplification and sequencing of a portion of the 16S rRNA gene. The genomic DNA (gDNA) was obtained using the Quick-DNA™ Fungal/Bacterial Miniprep Kit following the manufacturer's instructions. The quality and concentration of the gDNA were determined by electrophoresis in 1% agarose gel in Tris-Acetate-EDTA buffer (TAE: 40 mM Tris-HCl; 40 mM acetic acid; 1.0 mM EDTA, pH 8.0) added with DNA dye EZ-vision (Amresco; 5 µL/100 mL). The DNA samples (3 µL) were mixed with 0,5 µL of Blue Loading Buffer 6X (glycerol 30%, bromophenol blue 0.25%) before loading. The electrophoresis was run in a Mini-Sub® Cell (Bio-Rad), at 70 V for 45 minutes, after which the gel was observed in a ChemiDoc™ XR+ with the software Image Lab™ (Bio-Rad).

The 16S rRNA gene was amplified from the gDNA using primers 27F (5'-AGAGTTTGATCMTGGCTCAG-3') and 1492R (5'-TACGGYTACCTTGTTACGACTT-3') by the polymerase chain reaction (PCR) using a cycler MyCycler T100 (Bio-rad) and the program described in Table 3. The PCR mixture volume was 50 µL containing 25 µL of DFS-Taq Master Mix 2x, 0.4 µM of each primer and 2 µL DNA template.

Table 3. PCR program used for the application of the 16S rRNA gene

Step	Condition	
Initial denaturation	94 ºC, 2 min	
Denaturation	95 ºC, 10 sec	30X
Annealing	50 ºC, 20 sec	
Extension	72 ºC, 1 min	
Final extension	72 ºC, 5 min	

The PCR product was cleaned with the cleanup kit VWR® ExoCleanUp FAST, checked for quality and concentration by electrophoresis (as previously described) in 1.2% agarose gel, and sequenced by STAB VIDA Lda (Caparica, Portugal) in both directions using the same primers.

The resulting sequences were analyzed with the software BioEdit, and a consensus sequence was obtained using the program Sequencher 4.0. The consensus sequence was compared using the database GenBank from NCBI (National Centre for Biotechnology Information; http://www.ncbi.nlm.nih.gov/), using the BLAST (Basic Local Alignment Search Tool) algorithm. A phylogenetic tree was deduced after multiple alignment with 16S rRNA gene sequences of the type strains of each of the species in the *Komagataeibacter* genus with CLUSTAL W using the function "build" of ETE3 3.1.2 (Huerta-Cepas et al., 2016) as implemented on https://www.genome.jp/tools/ete/ and ML tree was inferred using PhyML v20160115 ran with model and parameters: --pinv e --alpha e --nclasses 4 -o tlr -f m --bootstrap -2 (Guindon et al., 2010). Branch supports are the Chi^2-based parametric values returned by the approximate likelihood ratio test. The sequences of all type strains from the genus *Komagataeibacter* were retrieved from the bacterial database BacDive (https://bacdive.dsmz.de/) and are listed in Table 4.

Table 4. Strain designation and GenBank accession numbers for sequences in 16S rRNA tree.

Name	Accession number	Strain Designation
Komagataeibacter maltiaceti	AB166744	NBRC14815
Komagataeibacter hansenii	AB166736	DSM5602
Komagataeibacter cocois	KR998072	CGMCC115338
Komagataeibacter pomaceti	MH355952	LMG30150
Komagataeibacter rhaeticus	AY180961	DSM16663
Komagataeibacter kakiaceti	AB607833	DSM24098
Komagataeibacter saccharivorans	AB166740	LMG1582
Komagataeibacter melaceti	MT422125	LMG31303
Komagataeibacter medellensis	JX013852	NBRC3288
Komagataeibacter intermedius	Y14695	DSM11826
Komagataeibacter oboediens	AJ001631	DSM11826
Komagataeibacter europaeus	Z21936	DSM6160
Komagataeibacter swingsii	AY180960	DSM16373
Komagataeibacter xylinus	AB205216	DSM6513
Komagataeibacter diospyri	MG971333	MSKU9
Komagataeibacter nataicola	AB166743	LMG1536
Komagataeibacter sucrofermentans	AJ007698	DSM15973
Komagataeibacter melomenusus	MT422127	LMG31304

3.2 Production of BC

3.2.1 Moist olive pomace

The MOP was collected at the olive oil extraction unit Olimontes (Macedo de Cavaleiros, Portugal), operating using a continuous two-phase centrifugation system. The samples were pasteurized at 75 °C for 30 min (Ecoline 012, Lauda, Königshofen, Germany) and cooled to 4 ºC for storage (H8 A1E W, Hotpoint-Ariston, Lisbon, Portugal) until use as a substrate.

3.2.2. Preparation of inoculum

The basic growth medium used for the culture was Hestrin and Schramm (HS) broth (20 g/L glucose, 5 g/L peptone, 5 g/L yeast extract, 2.7 g/L Na_2HPO_4, 1.15 g/L citric acid, H_2O) and the pH was adjusted to 5.7. The bacterial strain was precultured in 90 mL of HS medium in 250 mL flasks at 28 °C, at a static condition for 7 to 10 days in the incubator (SLN 240, POL-EKO, Wodzisław Śląski, Poland), a “seed inoculum” was obtained, which was used for a second inoculation. For this, two different ways were used, single colonies were used to inoculate the growth media or were inoculated with

10% of the previous fermentation. For BC production, a portion of the obtained fermentation broth containing cells and of the produced BC film was used in a proportion of 10% (v/v and w/v, respectively) as inoculum in 90 mL HS medium into 250 mL flasks and was incubated statically at 28 °C for 7 days. After two days of incubation, a thin gelatinous film was observed floating at the air-liquid interface (Figure 7).

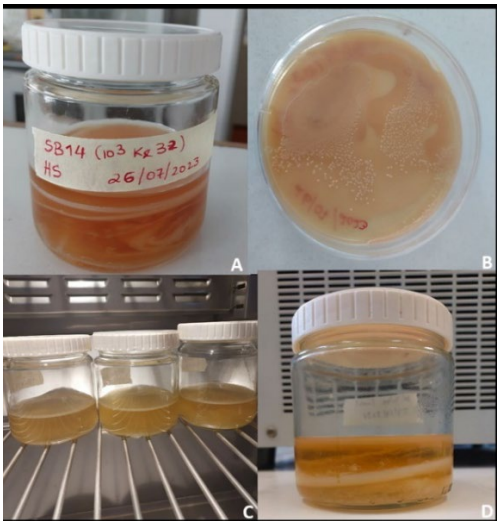

Figure 7. Cellulose production. (A) Seed inoculum; (B) Petri plate inoculated with the SB14 isolates; (C) Bacterial cellulose after two days of incubation in HS medium; (D) Bacterial cellulose after 7 days of incubation in HS medium.

3.2.3 Production of BC using moist olive pomace as substrate

The pasteurized MOP was mixed with HS broth in 250 mL flasks to obtain final different concentrations (1%, 5%, 10%, 20%, 30%, 40%) in 100 mL final volume (in triplicate). Control flasks were prepared in the same manner in the HS medium without the addition of MOP. The flasks were incubated for 7 days at 28 ℃ in a static condition (Figure 8). This step was carried out to evaluate BC production at different MOP concentrations.

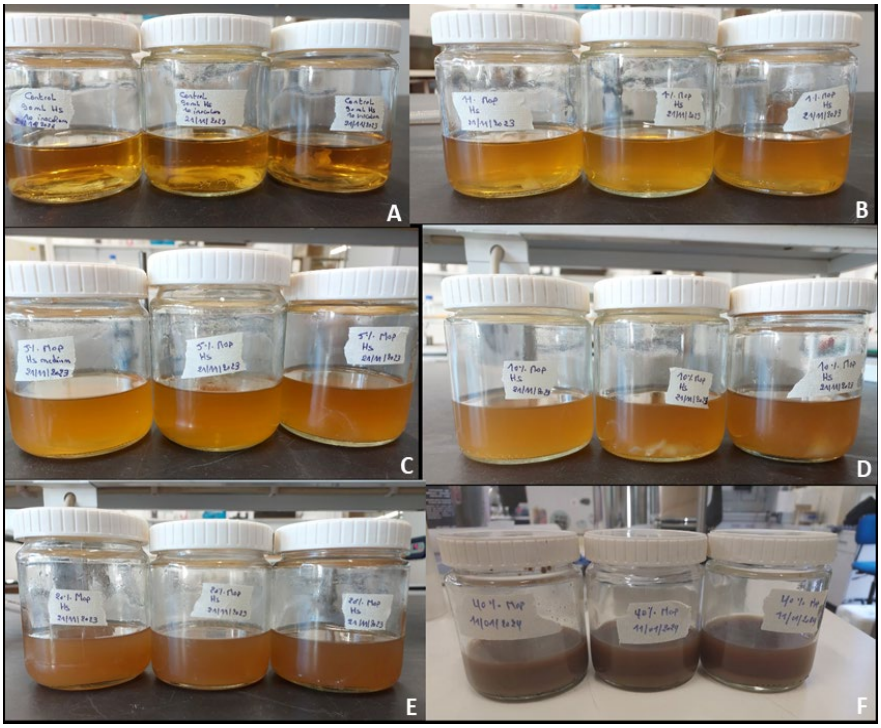

Figure 8. Preparation of broths with different MOP concentrations, for BC production. (A) control samples (HS); (B) HS+1% MOP; (C) HS+5% MOP; (D) HS+10% MOP; (E) HS+20% MOP; (F) HS+40% MOP.

3.2.4 Harvest and purification of BC pellicle

After incubation, the pellicles were removed from the flasks and were treated with 0.5N NaOH (JMGS, Portugal) at 50 rpm and 28 ℃ for 1h to eliminate cell particles or any type of residue. This step was followed by thorough washing with deionized water until a neutral pH 7 was achieved. After that, the cellulosic membranes were dried in a hot air oven by placing the pellicle in the oven at 28 ℃ until a constant weight was obtained (Figure 9). The weight measurement was carried out until the stable weight was reached to ensure that all of the water had been eliminated. The obtained dry weight was used to determine the mass of BC. The cell biomass was determined for each test condition by counting the colony-forming units per mL using the standard decimal dilutions and plate count method in Petri dishes containing 20 mL of HS agar.

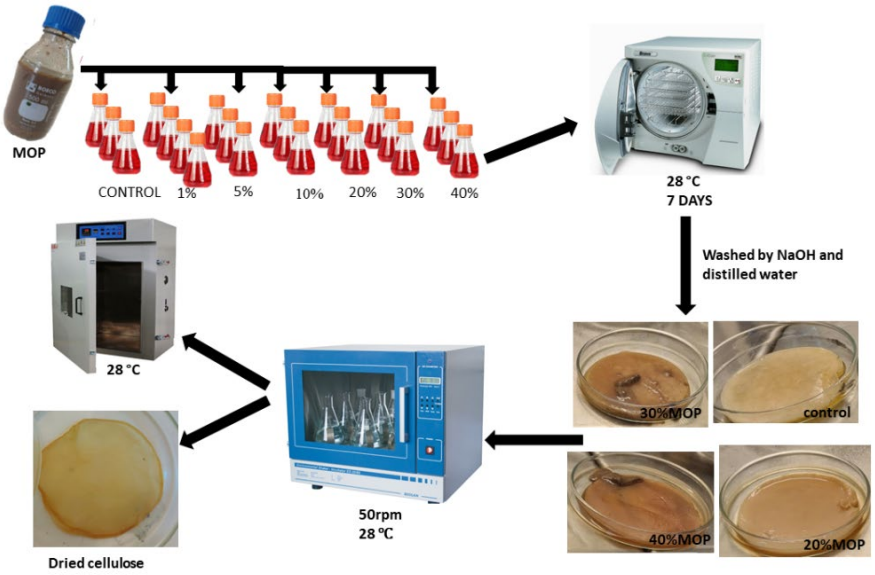

Figure 9. Scheme of the general procedure for obtaining dried cellulose.

3.2.5 Determination of glucose consumption by high-performance liquid chromatography (HPLC)

3.2.5.1 HPLC analytical conditions

The fermentation broths were analyzed for glucose before and after fermentation by high-performance liquid chromatography (HPLC). Before and after the fermentation process, broth samples of 1 mL were taken from each fermentation flask, filtered through 0.22 μm membranes to an Eppendorf and frozen until analysis. When needed the filtered samples were diluted in ultra-pure water and subjected to HPLC analysis.

The system was equipped with a pump (Varian Prostar 220), an injector (Rheodyne 7125), a refractive index detector and (Varian RI-4) was used and the column used to determine sugar concentration was a BIO-RED Aminex® HPX-87H, 300 mm x 7.8 mm column. The flow rate was set to a constant rate of 2.6 mL/min and the column temperature was set to 30 °C. The mobile phase used was sulfuric acid H_2SO_4 (4 mM) and the sample injection volume was set to 20 μL. The glucose standard for five levels of concentration (g/L) were used for the calibration curves and the data were analyzed using the Star Chromatography Workstation software (version 4.5).

3.2.5.2 Determination of method performance

Calibration curve, limit of detection (LOD), and limit of quantification (LOQ) were determined with five concentration levels of HPLC-grade standards of glucose ranging from 0.1 to 8 g/L. The curve equation was y = 2E+06x – 24691 and the R^2 = 0.9996 (Figure 10). LOD and LOQ were calculated as 0.24 g/L and 0.78 g/L, according to Taverniers et al. (2004). The concentration was calculated as g/L of glucose, considering the dilution factors.

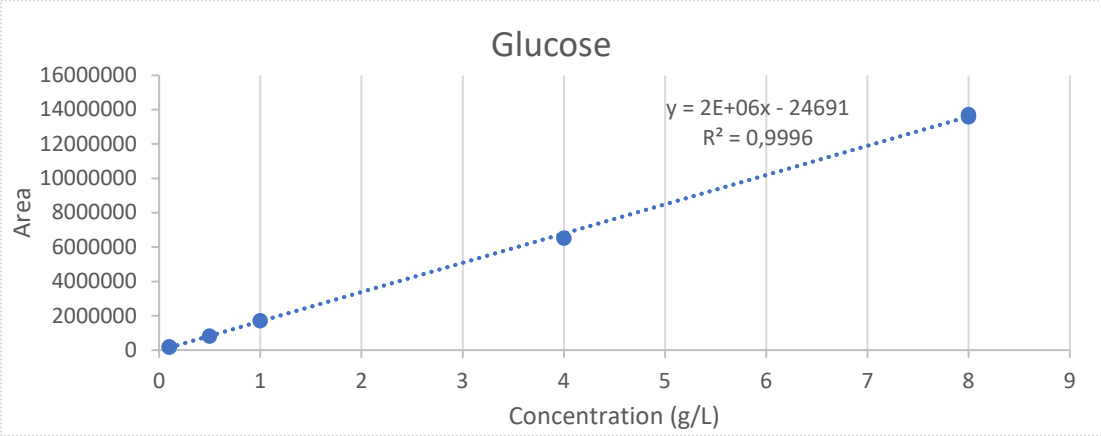

Figure 10. calibration curve of glucose measurement using the HPLC method.

3.2.5.3. Determination of fermentation yield

The BC yield, in gram of BC produced per gram of consumed glucose, was calculated using equation (1).

$$BC\ yield\ (g/g) = \frac{Dry\ weight\ (g/L)}{initial\ glucose\ (g/L) - final\ glucose\ (g/L)} \quad (1)$$

3.2.6 Irradiation protocols

The irradiations were carried out using a low-power LED device (Emilight, MMOptics, São Carlos, SP, Brazil) with a power of 100 mW at wavelengths of 630 ± 10 nm, depositing an energy density of 14 J/cm^2 continuously (Table 5). The irradiations were carried out on the bottom outside of the flask at an irradiation angle of 90° and a distance of 0.5 cm (Figure 11). The study groups, control, and 20% MOP were exposed to three consecutive applications every 24 hours after the first 24 hours of production.

Experimental samples were divided into two study groups (triplicates): irradiated group and non-irradiated group. All groups were subjected to the same conditions, including temperature, incubation duration, and radiation time.

Table 5. Light emission parameters used.

Parameters	LED
Wavelength (nm)	630 ± 10
Energy density (J/cm²)	14
Emission	CW
Spot size (cm²)	9
Power density (mW)	100

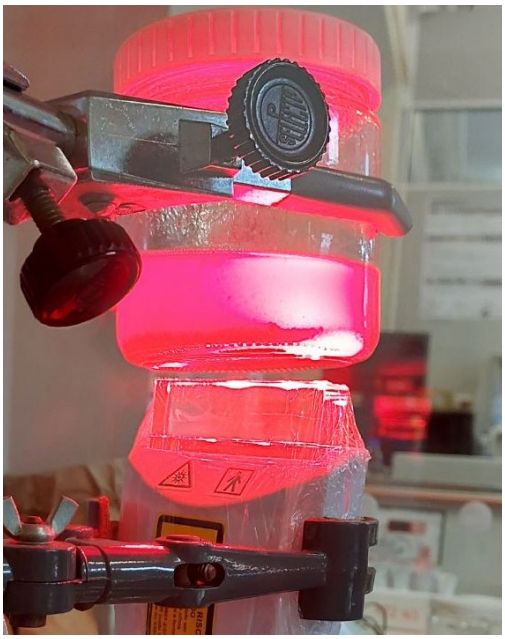

Figure 11. Irradiation setup with LED.

3.2.6.1 Microbial quantification

Quantification of the number of viable cells present in the collected samples after the irradiation protocols was carried out to assess the modulation effect of emitted red lights by inoculating 100 µL in Petri dishes containing HS agar medium, diluted 10 times so that no nutritional shock occurs. After an incubation time of 48-h at 28 °C, the quantification of cellular proliferation was achieved by CFU counting.

3.3 Characterization of the BC

3.3.1 Fourier transform infrared spectroscopy

Infrared analysis was performed on previously dried and purified BC on ABB MB 3000 spectrophotometer (Zurich, Switzerland) at 4 cm^{-1} resolution, between 4500 - 500 cm^{-1} at 32 scans/min (Figure 12). Spectra were acquired and processed using the software Horizon MB version 3.4. The background was acquired every two consecutive tests. For each BC sample, the spectra were acquired at several points (from 4 to 15) due to the heterogeneity of the surface, visible by visual inspection.

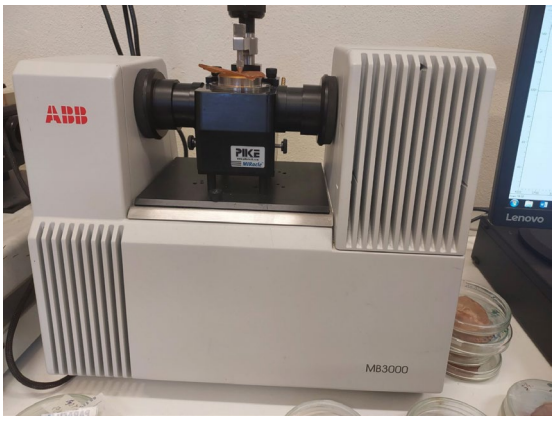

Figure 12. Fourier transform infrared equipment.

3.3.2 Thermogravimetric analysis (TGA)

The thermal stability of BC films was analyzed using a NETZSCH - TG 209 F3 Tarsus (Netzsch, Selb, Germany) thermogravimetric analyzer. The polysaccharides were heated from 25 to 800 °C, at 10 °C/min in alumina crucibles (7 mg) under an inert nitrogen atmosphere with a flow rate of 50 mL/min. Thermogravimetric (TG) and thermogravimetric derivative (DTG) curves were obtained using Netzsch Proteus thermal analysis software (v.5.2.1).

3.3.3 Mechanical properties of the BC membranes

The mechanical tensile tests were carried out using a static-dynamic miniature testing machine (Shimadzu Autograph AGS-X Series, Kyoto, Japan) equipped with a 10

kN load cell and pneumatic clamps to fix the samples. For each sample, pieces of the BC membranes with dimensions 15 ×30 mm were cut. At least 3 tests were conducted for each membrane with a crosshead speed of 5 mm·min^{-1} at room temperature. From these tensile tests, mechanical properties such as the tensile strength, strain at break, and Young's modulus (elastic modulus), were determined. The tensile modulus of a solid material is a mechanical property that measures its stiffness. It is defined as the ratio of its tensile stress (force per unit area) to its strain (relative deformation) when undergoing elastic deformation. The differences in the mechanical behavior between studied membranes were obvious. The more pronounced differences were the higher tensile strength and Young's modulus expressed by the following equation (2):

$$E = \sigma/\varepsilon \qquad (2)$$

where ε is the tensile strain in the material (extension/original length) and σ the tensile stress in the material.

3.3.4 Biological properties

3.3.4.1 Antioxidant activity

Antioxidant capacities of BC membranes were measured by DPPH radical scavenging activity assays. First, the membranes were divided into small pieces (10 mg) and placed in test tubes with 1 mL of DPPH solution prepared at a concentration of 6x10^{-5} M for 30 minutes in the dark at room temperature. At the end of incubation, samples were measured using a UV-spectrophotometer (BioTek EPOCH 2 microplate reader, USA) at 517 nm wavelength. The test was carried out in triplicate and the results were given as a percentage using equation (3):

$$Inhibition\ (\%) = \frac{A_i - A_f}{A_i} \times 100 \qquad (3)$$

where A_i is the absorbance value of DPPH while A_f is the absorbance value of the BC samples.

3.3.4.2 Antimicrobial activity tests

Antimicrobial susceptibility tests were done on Mueller-Hinton (MH; Himedia, India) using the disk diffusion method to determine the antimicrobial activity of the BC pellicles produced using the different MOP-based substrates. The pellicles were tested for reference strains of *Escherichia coli* ATCC 25922 (Gram-negative bacterium), *Staphylococcus aureus* NCTC 10788 (Gram-positive bacterium), *Candida albicans* ATCC 2091 (yeast) and *Aspergillus brasiliensis* ATCC 16404 (filamentous fungus). Cell suspensions of the bacteria and yeast were prepared in BHI broth (Panreac, Spain) at 37 °C, for 24 h under aerobic conditions, then diluted using sodium chloride (0.9%) solution to obtain turbidity equivalent to 0.5 in McFarland scale. For *A. brasiliensis*, a spore suspension at the concentration of 1 x 10^6 spores/mL was prepared in distilled water with Tween (0.5%) using a Neubauer-improved counting chamber. Each cell or spore suspension was swabbed on square plates (120 x 120 mm) containing 20 mL of MH agar medium.

After that, 5 mm diameter discs were cut from each dried pellicle (control, 1% MOP, 5% MOP, 10% MOP, 20%, 30% MOP, and 40% MOP) under sterile conditions and placed on the inoculated plates as shown in Figure 13. Discs of the antimicrobials nitrofurantoin, penicillin, flucytosine, and amphotericin B were used as positive controls with strong activity against *E. coli*, *S. aureus*, *C. albicans,* and *A. brasiliensis*, respectively. Discs of amoxicillin, ampicillin, and amphotericin B were also used as controls with lower activity against *E. coli*, *S. aureus*, and *C. albicans*, respectively.

Antimicrobial activity was determined by measuring the diameter of the inhibition halo produced by each film for each microorganism, after incubation at 37 ºC for 24 h for *E. coli* and *S. aureus*, 37 ºC for 48 h for *C. albicans* and 28 ºC for 5 days for *A. brasiliensis*.

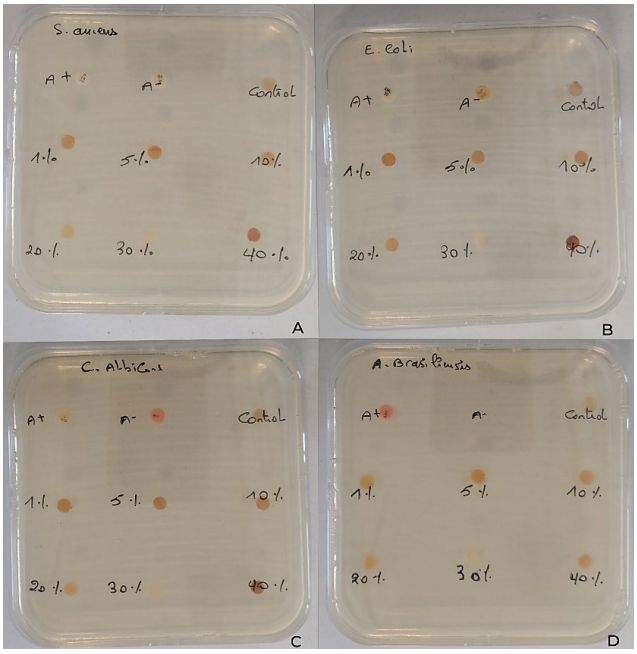

Figure 13. Disk diffusion test plates for antimicrobial activity of BC. (A) and (B): antibacterial activity against *S. aureus* and *E. coli,* respectively. (C) and (D): antifungal activity against *C. albicans* and *A. brasiliensis* respectively. (A+ and A-: highly active and less active antimicrobial discs, respectively; Control: HS medium only; percentages (1%, 5%, 10%, 20%, 30%, and 40%): MOP concentration used for the fermentation).

3.4 Statistical analysis

The results obtained in the different tests were analysed using ANOVA statistical test with Tukey's multiple comparison post-test using the GraphPad Prism® 8.0 software (San Diego-CA, USA).

4. RESULTS AND DISCUSSION

4.1. Identification of cellulose-producing strain

By visually observing the bacterial colonies on HS agar plates, the morphologies of the colonies were described. The growth of colonies confirmed that the isolated bacteria *SB14* were able to grow on HS medium and displayed a circular convex shape with a milky white color and smooth texture. Further, differential Gram staining of the isolated bacteria was performed and was found to be a gram-negative strain as shown in Figure 14.

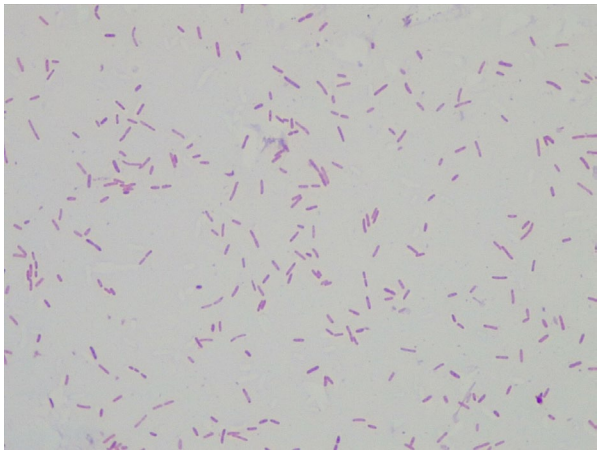

Figure 14. Gram staining of the isolate *SB14*.

For the bacteria's molecular characterization, the conserved and hypervariable areas found in the bacterial kingdom are known to be found in the 16S rRNA gene. As a result, it serves as a genetic identifier and facilitates our understanding of the taxonomy and phylogenetic relationships of bacteria (Gayathri, 2020). By analyzing the 16S sequence, the bacterial strain *SB14* was identified as *Komagataeibacter intermedius*. As evidenced in Figure 15, the species of this genus are grouped phylogenetically into cellulose-producers such as *K. xylinus, K. swingsii, K. rhaeticus, K. nataicola, K. cocois, K. diospyri, K. kakiaceti, K. nataicola, K. sucrofermentans,*and *pomaceti* (Ryngajłło et al., 2020). The strain *SB14*, which exhibits this characteristic, clustered also with the 'cellulose-producing' group, and specifically with the branch formed by *K. intermedius* DSM11804^{T} with 99.98% similarity.

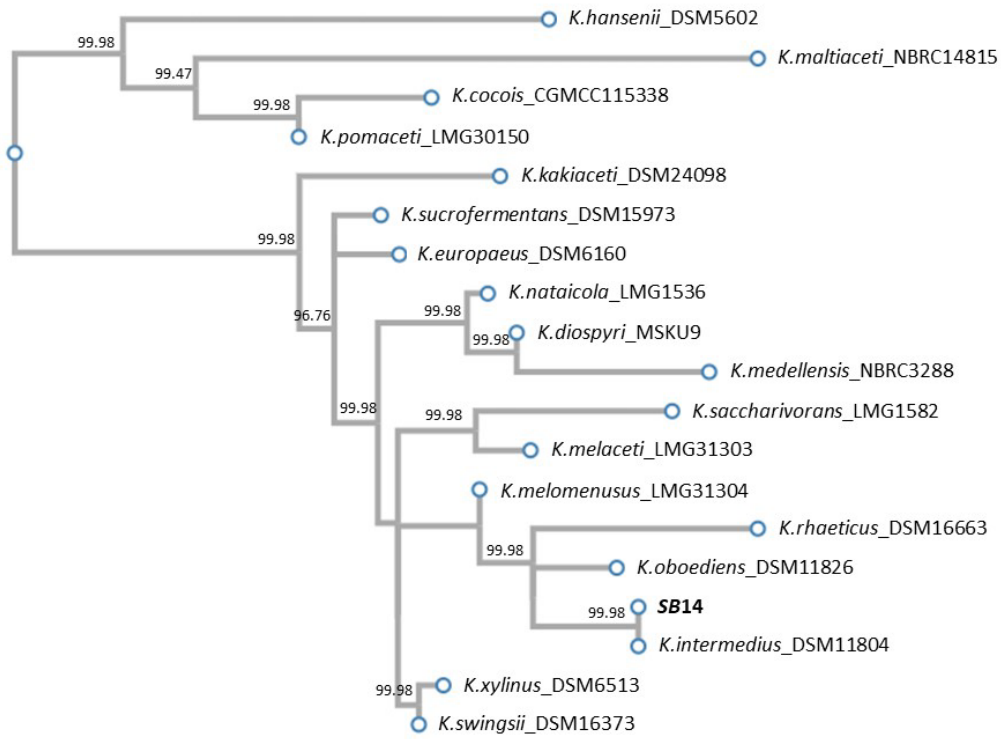

Figure 15. Phylogenetic tree of the strain SB14, representing its relative position in the genus *Komagataeibacter* based on 16S sequences.

Komagataeibacter intermedius is commonly found in fruit juice, wine vinegar, and Kombucha. It is well known for using mannitol as the only carbon source to produce BC (Devanthi et al., 2021). Lin et al. (2016) reported that *K. intermedius* and *K. xylinus* both exhibited similar BC production capability at pH 4 and 5 in the short-term cultivation (4 days). However, *K. intermedius* was able to produce more BC than *K. xylinus* in the range of pH 6-8 (Lin et al., 2016). *Komagataeibacter intermedius* produced BC free from impurities, with a high crystallinity index, and similar mechanical properties to the one produced by *K. xylinus* (Devanthi et al., 2021).

4.2. Effect of moist olive pomace on BC production

The dry weights were recorded for all the experimental conditions and represented as mean ± standard error allowing us to determine BC yield as illustrated in Figure 16. It was observed that the addition of MOP significantly increased BC production ($p < 0.0001$) with 21.7% for 1% MOP and 154.78% for 10% MOP compared to the control

samples. The highest level of biosynthesis was obtained at 20% MOP reaching 6.2 g/L. However, the BC yield with 30% MOP and 20% MOP was significantly different ($p < 0.0001$) compared to that obtained in the fermentation with 10% MOP and 20% MOP ($p \leq 0.05$). This result supports that industrial waste can have a potential effect on bacteria to produce BC. Lestari et al. (2014) also used the waste coconut water as a nutrient source for the fermentation, it was observed that the conversion of glucose into cellulose biomass was higher with higher BC production. The finding result indicated that the phenolic components found in MOP might also act as a stressor for microorganisms to produce an increased yield of BC (Urbina et al., 2021). A study by Crugeira et al. (2023) also showed that the stress caused by the phenolic compounds present in MOP caused the bacteria to develop a defense mechanism against adverse conditions, increasing the production of xanthan gum by *Xanthomonas campestris.* Compared to another study conducted by Gomes et al. (2013), BC obtained using dry olive mill residue (DOR40, DOR100) was in lower yields (0.81±0.04 g/L, and 0.85±0.04 g/L, respectively) than those reported with the reference medium HS (2.5 g/l). Thus, we found out that MOP in the HS medium is more efficient in producing BC.

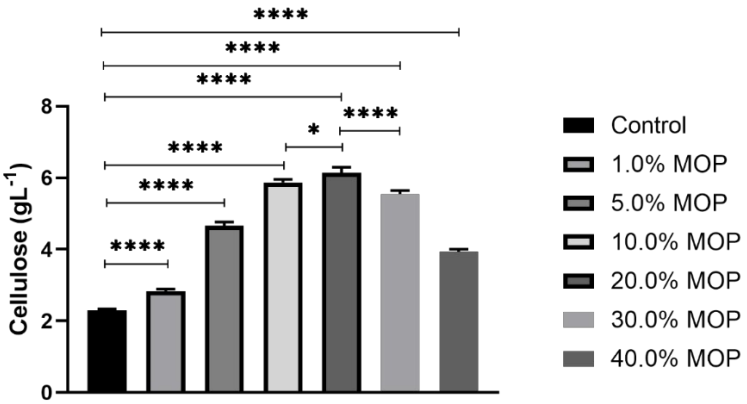

Figure 16. Effect of different MOP concentrations on the yield of bacterial cellulose after 7 days of fermentation. The significant differences are indicated by * ($p \leq 0.05$) and **** ($p \leq 0.0001$).

BC yield is calculated as the amount of BC produced (in g) by each gram of glucose, and reflects the rate of conversion of a substrate into a product. This parameter allows to determine and discuss the efficiency of a bioprocess. BC yield was calculated for each fermentation condition – HS basal medium as control and HS added with different concentrations of MOP - by plotting the dry weight of each BC against the

amount of glucose consumed. Figure 16 shows that *K. intermedius* consumed the highest amount of glucose (9.5 ± 1.52 g/L) in the basal HS medium, but that was also the condition where the amount of BC was the lowest (2.30 ± 0.01 g), resulting in a very low yield (0,24 ± 0.04 grams of BC produced for each gram of glucose consumed). The highest yield was achieved in the 5% MOP (0,89 ± 0.18 g/g), reflecting a high conversion rate, but the amount of BC produced was not optimal. Given these results, the use of 20% MOP is the best condition for BC production, even though it is not the best in terms of yield.

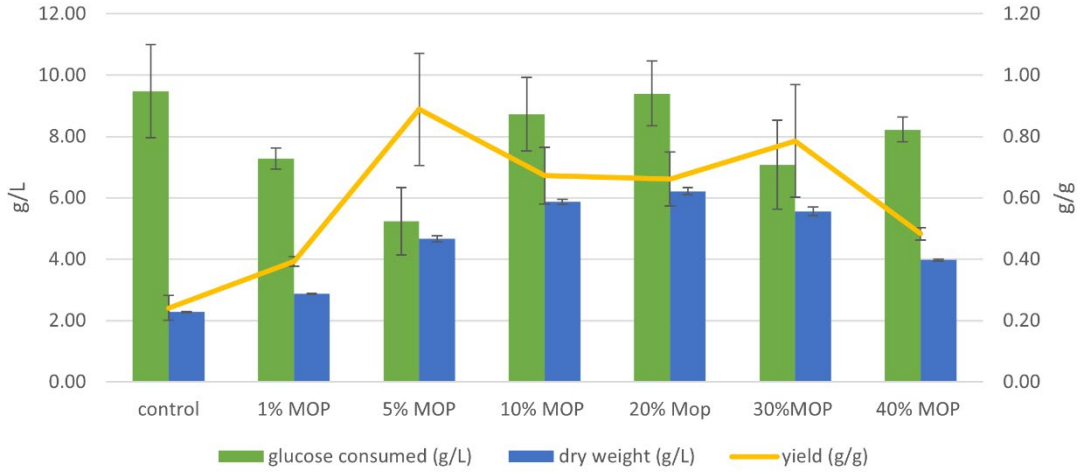

Figure 17. Dry weight (g/L) of the bacterial cellulose, glucose consumption (g/L), and the BC yield by substrate (g/g).

4.2.1. Effect of LED irradiation on BC production

4.2.1.1. BC production

Considering the results obtained in the previous assay, the irradiation of samples with 20% MOP was chosen because our study aims to use the highest concentration of waste resulting in the highest production of cellulose. The information summarized in Figure 18 is the BC produced from all tested groups (irradiated group, non-irradiated group) after 7 days of incubation. A significant increase in BC production of 124% was observed for the control LED group ($p < 0.001$) and 392% for the 20%MOP+LED group $p < 0.0001$), compared to the control group. These results can be explained that red light can stimulate the microorganisms to produce more BC. A study by Pinheiro et al. (2020) also reported that photo-stimulation with LED increased Xanthan gum production in bacterial cultures. In the 20%MOP+LED group, where bacteria were exposed to dual

stressors, two distinct responses were observed. Firstly, the *K. intermedius* engaged in self-protection by increasing exopolysaccharide production. Secondly, they responded to photobiomodulation stress, corresponding to two hypotheses. The first hypothesis suggests that photoexcited cytochrome oxidase leads to increased ATP utilization by *K. intermedius* for multiplication. Alternatively, light may activate enzymes within the cellulose biosynthetic pathways. cytochrome c oxidase is the essential component of the respiratory electron transport chain in bacterial cells. It is one of the red spectrum irradiation targets. When photoexcited, this protein complex enhances its proton-pumping capacity, which increases the amount of cellular ATP that is accessible (Passarella & Karu, 2014).

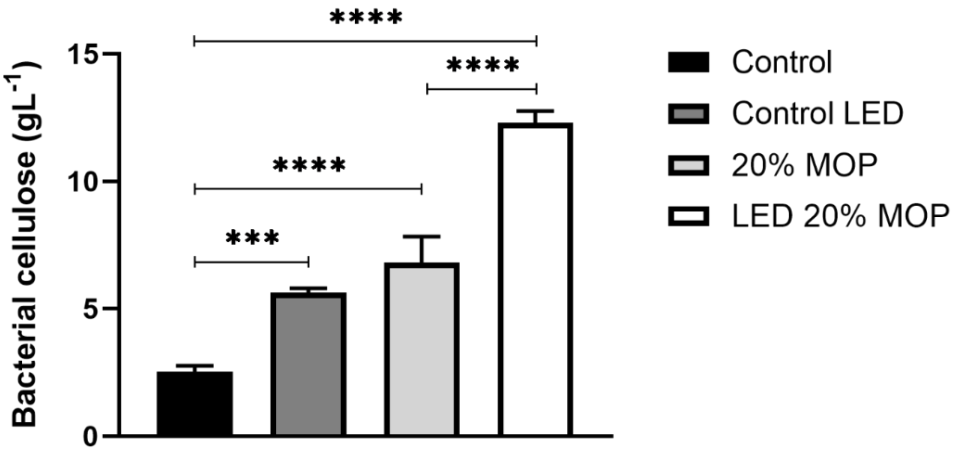

Figure 18. Effect of the photobiomodulation by LED irradiation with (λ= 630±10) on the BC production after 7 days of fermentation. The significant differences are indicated by * (p≤ 0.05) and **** (p≤ 0.0001).

4.2.1.2. Microbial growth monitoring

The microbial growth of *K. intermedius* was carried out after 24, 48, and 72 hours. showed an increasing cell count for all groups in direct proportion to the time (Figure 19). There was an increased growth in the irradiated group compared to the non-irradiated group. After 24h an increase in microbial growth was observed for the LED control group and 20%MOP+LED group with ($2.3X10^7$ UFC/ml and $2.1X\ 10^7$ UFC/ml, respectively) compared to the control group ($1.7X10^7$ UFC/ml). After 72h the microbial growth increased by 17.99% and 9.52 % for the LED control group and 20%MOP+LED group, respectively compared to the control group. This is though not in accordance with the BC production, where 20% MOP+LED resulted in the highest BC production The findings result on the multiplication of post-irradiation microorganisms suggest that ATP-induced

activation of the DNA A protein may be the reason for this. It is well known that exposed cells have higher levels of cellular ATP. The start of microbial replication is made possible by the binding of this active DNA A/ATP protein complex to the OriC sequence in the microbial genome (Crugeira et al., 2018). The hypothesis that may explain the higher growth of microorganisms for the LED control group compared to the 20% MOP+LED group, is that the increased BC production for this group depends on the enzymes stimulated within the biosynthesis pathway, rather than being resulted by microbial multiplication.

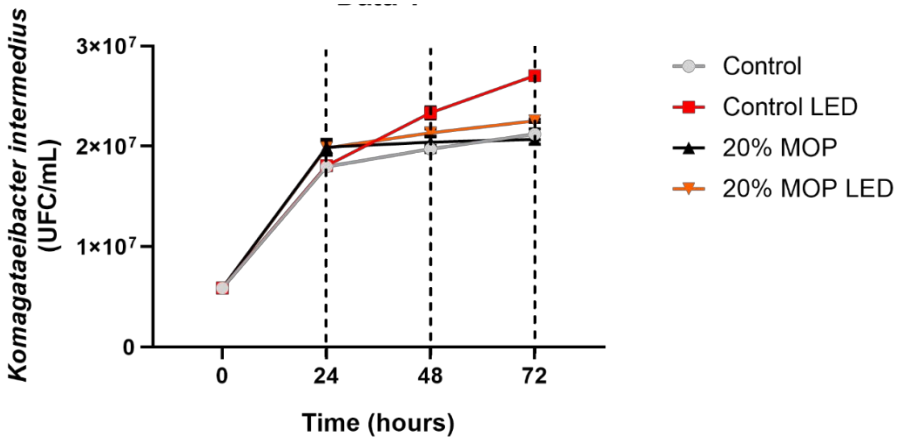

Figure 19. Bacterial growth monitoring of viable cells every 24 h up to 72h for the irradiated group and non-irradiated group.

4.3. Characterization of BC produced with MOP and LED

4.3.1. FTIR characterization

4.3.1.1. BC-MOP films

The FTIR spectra, acquired in the range of 4000–500 cm^{-1}, provided insights into the molecular structure and the corresponding physical-chemical properties. As depicted in Figure (20. a), the FTIR spectra of BC films exhibited a pattern analogous to that of microcrystalline cellulose (MCC) (Aldrich, Portugal) and moist olive pomace spectra (Figure 20. b), With slight variations in intensity at specific peaks. The characteristic peaks related to cellulosic structure appear in MCC at 662, 895,1020 cm^{-1} were also present in all BC films where the absorption band at 895 cm^{-1} is attributed to C-H rocking vibrations (anomeric vibration specific to β-glycosidic linkage) (Abu-Thabit et al., 2020) and the peaks in the region of 1000 to 1200 cm^{-1} are indicative of the C=O groups in the primary hydroxyl strong stretching vibration (Almeida et al., 2022). The 1600–1500 cm^{-1}

band is ascribed to the presence of an aromatic C–C ring stretching (Bohli et al., 2015) presented in all samples with more intensity in 20% MOP film. The band corresponding to the symmetrical stretching vibration of CH2 (Haydari et al., 2022) was observed at 1380 cm^{-1} in MOP. This feature was also present in all BC films, appearing at 1410 cm^{-1} in the BC film with 20% MOP and at 1380 cm^{-1} in the control sample. The band at 1740 cm^{-1} seen in BC films produced with 5%, 20%, 30%, and 40% MOP is associated with C = O, which may be related to the fatty acids and this can be interpreted as tyrosol and hydroxytyrosol naturally (Sar & Yesilcimen Akbas, 2022) found in MOP may be absorbed into the cellulose samples. The two distinct sharp bands at 2920 and 2850 cm^{-1} are indicative of C–H stretching vibrations (Vadanan, 2020), while the peak at 2359 cm^{-1} is associated with C=N stretching (Bohli et al., 2015). These features were observed in both MOP and the BC films but were absent in the microcrystalline cellulose (MMC) as shown in Table 6. The peak of 3340 cm^{-1} attributed to the intermolecular and intramolecular hydrogen bonds (Fernández et al., 2019) exhibited stronger peak intensities in the BC membrane with 10% MOP, 20 MOP, and 30% MOP compared to the other films. However, A high-frequency shoulder in the MMC at around 3400 cm^{-3} indicates that there is a large concentration of cellulose I_β is a sub-allomorph of Cellulose I, characterized by its monoclinic microfibrillar arrangement, vascular plants and wood cellulose predominantly contain cellulose I_β (Gayathri, 2020). It was also observed a peak at 3327 cm^{-1} in MOP indicates the OH stretching vibration mode in alcohol and phenol (Aslan & Şirazi, 2020).

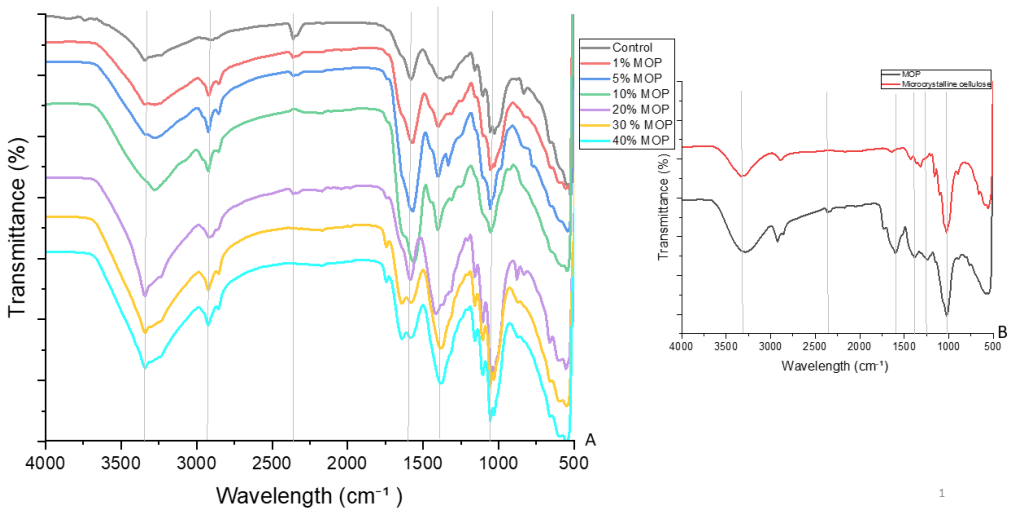

Figure 20. Fourier-transformed infrared spectra. (A) Control film and BC-MOP film spectra; (B) microcrystalline cellulose and the moist olive pomace spectra.

Table 6. Comparison of peaks and their assignments.

Cellulose Peaks	Assignments	MOP peaks	Assignments	BC peaks	Assignments
662 cm^{-1}	O-H out of plane bending			662 cm^{-1}	O-H out of plane bending
895 cm^{-1}	C-H rocking vibration	895 cm^{-1}	C-H rocking vibration	895 cm^{-1}	C-H rocking vibration
1000-1200 cm^{-1}	C-O-C stretching	1020 cm^{-1} 1228 cm^{-1}	C-O-C stretching CH2 wagging mode	1026 cm^{-1}	C-O-C stretching
1425 cm^{-1}	CH2 bending	1380 cm^{-1}	H-C-H stretching	1380 cm^{-1}	H-C-H stretching
1694 cm^{-1}	O-H stretching	1500-1600 cm^{-1}	C-C stretching	1580 cm^{-1} 1740 cm^{-1}	C-C stretching C=O stretching
2843 cm^{-1}	C-H stretching	2359 cm^{-1} 2850/2950 cm^{-1}	C=N stretching C-H stretching	2359 cm^{-1} 2850/2950 cm^{-1}	C=N stretching C-H stretching
3340 cm^{-1}	O-H stretching	3327 cm^{-1}	O-H stretching	3340 cm^{-1}	O-H stretching

4.3.1.2.BC-LED films

The FTIR spectra are presented in Figure 21 to identify the functional groups of the irradiated and non-irradiated BC membranes. A broad absorption peak of –OH stretching vibration at 3340 cm^{-1} due to the intermolecular hydrogen bonds was observed in all membranes (Almeida et al., 2022). The two small, sharp bands at (2920 and 2850 cm^{-1}) and the peak at 1740 cm^{-1}, which correspond to C–H (Vadanan, 2020) and C–O stretching group (Sar & Yesilcimen Akbas, 2022), respectively, appeared in all BC films with less intensity in the control LED sample. The peak around 2359 cm^{-1}, which corresponds to the C=N stretching (Bohli et al., 2015), was also present in all the samples. The peak is associated with the presence of an aromatic C–C ring stretching that occurs at 1580 cm^{-1} (Bohli et al., 2015) being less intense in the LED group samples compared to the control samples. The bands at 1380 cm^{-1} and 1050 cm^{-1} attributed to the symmetrical stretching vibration CH2 (Haydari et al., 2022) and the C=O groups in the primary hydroxyl strong stretching vibration (Almeida et al., 2022), respectively. Were less intense in the LED 20% MOP group. These results indicate that certain peaks shift

less intensely after the irradiation which could be due to changes in the vibrational energy levels of the molecules in the BC membrane.

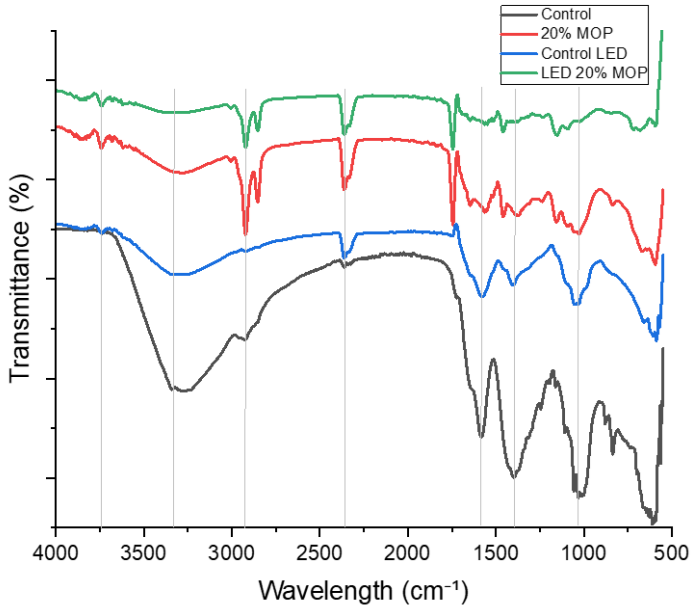

Figure 21. Fourier-transformed infrared spectra of bacterial cellulose membranes after LED irradiation.

4.3.2. Thermal properties

4.3.2.1. Thermal properties of BC-MOP film

The measurement of TGA relies on two major factors, namely mass change and temperature change, and the derivative (DTG) curves are shown in Figure 22, all samples showed a first mass loss stage (50–180 °C), which was linked to moisture desorption and the breaking of the water hydrogen bonds of the polar groups (-OH) in polysaccharides (Crugeira et al., 2023). Notably, the 5% and 20% samples demonstrated a higher mass loss (20%), suggesting these samples retained more water compared to others. The second thermal event for the BC control, occurring between 160-210 ºC and resulting in a 15.89% weight loss, is likely due to the cleavage of glycosidic bonds within the polymer (Gayathri, 2020) with peak degradation at 193.5°C (Table 7). For BC-MOP films (1%, 5%, 10%, 20%, 30%, 40%), degradation occurred in the range of 210-300°C, with an average mass loss of 24% and maximum degradation at 270°C. This contrasts with the control film, which showed an 18.5% weight loss and a peak at 297°C, indicative of the

release of small molecular fragments like hydroxyl and methyl hydroxyl groups(Cheng et al., 2009). In comparison, microcrystalline cellulose exhibited a significant weight loss of 77% at 350°C (Figure 21.b). This result indicates that BC produced in the presence of MOP presented lower thermal stability compared to the BC produced in the HS medium, attributed to structural changes caused by using MOP as substrate.

Table 7. Peak temperature of DTG.

	peaks (°C)			
Microcrystalline celluose	65.3	-	-	339.7
Control	84.8	-	193.5	297
1% MOP	75.1	161	-	269
5% MOP	63.3	-	-	269.5
10% MOP	60	161.1	-	270.8
20% MOP	66.1	-	-	273.2
30% MOP	139.2	-	-	268.7
40% MOP	58.2	141.1	-	260.8

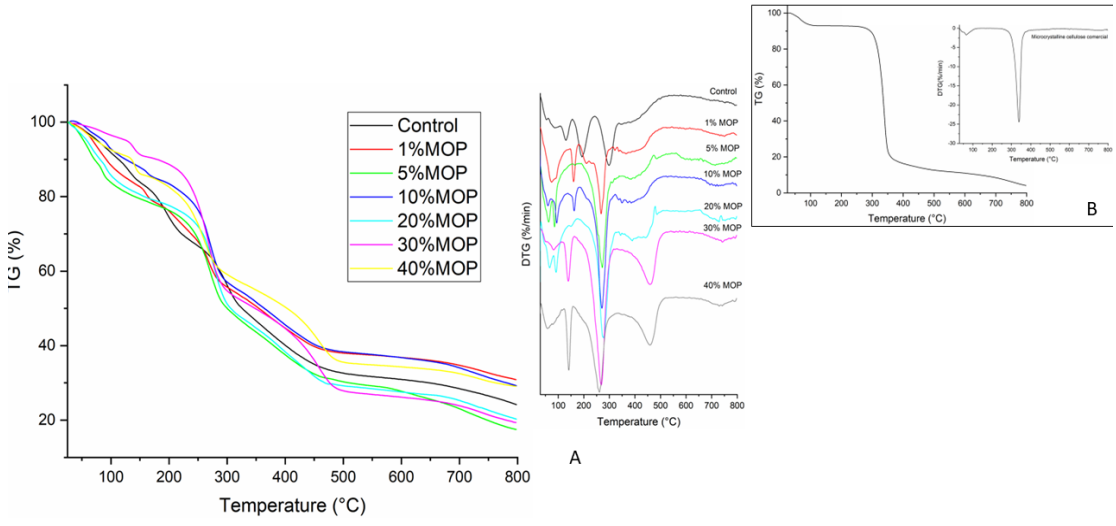

Figure 22. TGA and DTG thermograms. (A) BC-MOP films; (B) Microcrystalline cellulose.

4.3.2.2.Thermal properties of BC-LED film

The TG/DTG analyses depicted in Figure 23 reveal that the initial weight loss stage (50–180 °C) for both irradiated and non-irradiated BC films correspond to the dissociation of hydrogen bonds between water molecules and the polar groups (-OH) in polysaccharides (Crugeira et al., 2023), however, the LED 20% MOP samples exhibited a higher mass loss (50.9%), suggesting a more capacity to retain water compared to other samples. The peaks attributed to the degradation of the polymer occurred at 270.8°C with 36% weight loss in the LED 20% MOP group and at 273.2°C with 18.3% weight loss for the non-irradiated (20% MOP) group. The results indicate that irradiation makes BC films less thermostable.

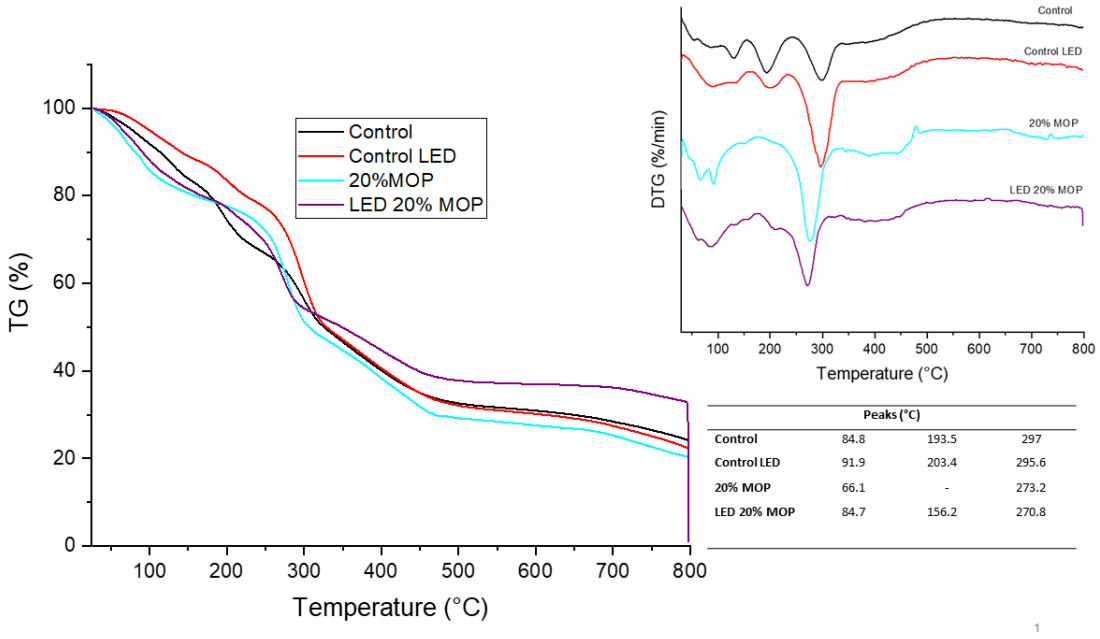

Peaks (°C)			
Control	84.8	193.5	297
Control LED	91.9	203.4	295.6
20% MOP	66.1	-	273.2
LED 20% MOP	84.7	156.2	270.8

Figure 23. TGA and DTG thermograms of irradiated BC films.

4.3.3. Mechanical properties

The mechanical behavior of the BC membranes was investigated in order to observe the variations resulting from the addition of MOP since their properties depend on the producing strain as well as the fermentation conditions (Tsouko et al., 2015). For instance, the degree of crystallinity of BC strongly influences its mechanical properties

(Almeida et al., 2022). The tensile test results for each of the BC membranes are shown in Table 8, where the average values of young's modulus, tensile strength, and deformation. There was a significantly higher stress in the cellulose produced with 20% MOP (60.732 MPa) compared to the other samples, with the 5, 30, and 10% MOP study groups being extremely close. The 5 and 20% MOP samples showed greater deformation capacity, with values of 0.722 and 0.696, respectively (Figure 24).

The BC membrane produced with 40% MOP showed a lower deformation capacity, i.e. elasticity, compared to the control group. On the other hand, the BC produced with 1% MOP showed less resistance to the force applied compared to the control. The control BC samples attained a value of Young's modulus (129.25 MPa), while for the 30% and 40% samples, this value increased to 153.72 MPa and 179 MPa, respectively (Figure 25). Similar mechanical properties have been described for the BC membrane with HS medium (Tsouko et al., 2015).

Table 8. Mechanical properties of BC membranes.

BC membranes	Young's modulus (MPa)	Tensile strength (MPa)	Deformation (m/m)
Control	129.25	12.757 ± 0.45	0.098±0.31
1% MOP	63.78	9.09± 0.42	0.142±0.24
5% MOP	34.015	24.559± 0.54	0.722±0.33
10% MOP	54.72	23.476±0.34	0.429±0.30
20% MOP	87.26	60.732±0.29	0.696±0.18
30% MOP	153.72	23.673±0.28	0.154±0.34
40% MOP	179	10.740±0.36	0.06±0.49

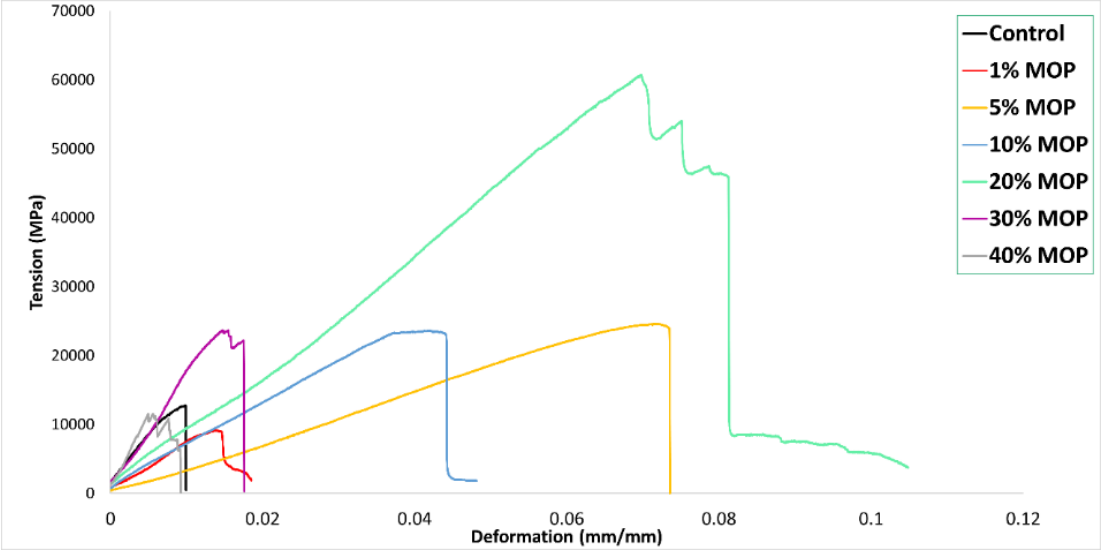

Figure 24. tension-deformation curves obtained in the tensile tests for BC membranes.

4.3.4. Biological properties

4.3.4.1. Antioxidant activity

Figure 25 shows the kinetics of the percent of radical inhibition of BC samples. The radical scavenging activity of the control sample was recorded as 3.071%, i.e. a relatively low antioxidant activity. However, the addition of different concentrations of MOP resulted in an improvement in antioxidant activity, reaching the highest value of 39.13% for 20% MOP with statistical significance of $p < 0.0001$ in relation to the control. In any case, there was no statistical difference between the 20 and 30% MOP group. The antioxidant activities of BC-MOP samples could be due to the presence of organic acids and bioactive phenolic compounds in the membranes that could be incorporated from the culture medium (Dima et al., 2017). According to Cabañas-Romero et al. (2020), it was found that previous studies demonstrated that BC contains aldehyde groups and that these groups have antioxidant properties, also showed that the chitosan impregnated with BC increased the antioxidant activity.

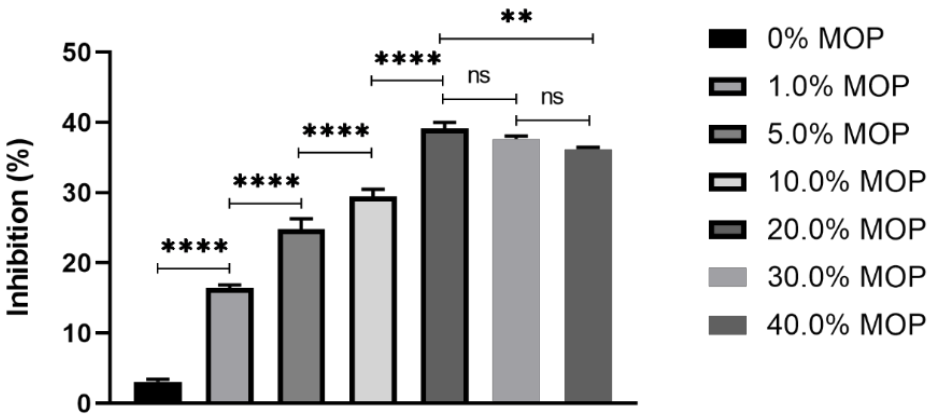

Figure 25. DPPH free radical scavenging activity of BC samples.

4.3.4.2. Antimicrobial activity

The antimicrobial activity was measured based on the diameter of the zone of inhibition. The antimicrobials nitrofurantoin, penicillin, flucytosine, and amphotericin B exhibited greater inhibitory for *E. coli*, *S. aureus*, *C. albicans*, and *A. brasiliensis*, respectively, as expected. No inhibition zone was observed for the BC films, for all microorganisms (Figure 26). In a similar study, Gayathri, (2020) performed the antimicrobial activity of BC and reported that microbial growth was not inhibited on control plates having only BC discs. This result indicates that BC naturally lacks antimicrobial activity, at least under the studied conditions. Some modifications such as the addition of polymeric materials or nanoparticles could improve the antimicrobial activity of BC. As reported by Cabañas-Romero et al. (2020), BC−chitosan composites inhibit microbial growth by direct contact of the microorganism with their surface.

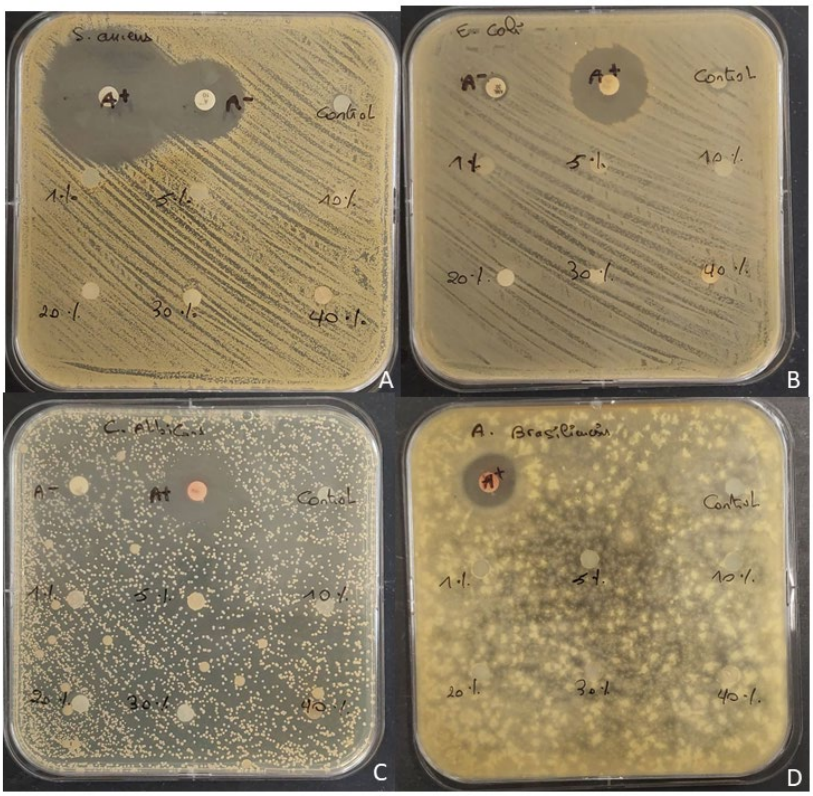

Figure 26. Antimicrobial activity of BC films. (A) and (B): antibacterial activity against *S. aureus* and *E. coli,* respectively. (C) and (D): antibacterial activity against *C. albicans*, and *A. brasiliensis* respectively. (where A+ and A- stand for highly active and less active antimicrobial discs, respectively; Control represents HS medium only, and the various percentages (1%, 5%, 10%, 20%, 30%, and 40%) reflect the MOP concentration used for the fermentation).

5. CONCLUSIONS

In this study, we investigated BC produced by *K. intermedius* using MOP and photostimulation. Our findings revealed that moist olive pomace (MOP) significantly enhanced BC yield (g/L) by 166.9% when 20% MOP was used compared to control samples. The presence of phenolic compounds in MOP-induced BC production highlights their ability to induce stress. Additionally, LED photostimulation (λ= 630 ± 10 nm) increased cellular proliferation, protein production, and metabolic activity boosting BC production.

Both the LED control group and the LED 20% MOP group showed a higher BC production (124% and 392%, respectively) compared to the control. The BC films produced from MOP and LED irradiation presented the characteristic BC functional groups and good thermal stability. The addition of MOP enhances the mechanical properties and the antioxidant activity of BC. The results are encouraging to get the BC synthesized in an economical way that can be applied for beneficial purposes e.g., biomedical applications, and cosmetics.

6. PATENT

inpi instituto nacional da propriedade industrial

INSTITUTO POLITÉCNICO DE BRAGANÇA
CAMPUS DE SANTA APOLÓNIA
5300 - 253 BRAGANÇA

Direção de Marcas e Patentes
Departamento de Patentes e Modelos de Utilidade

Ref. DP/01/2024/82212	PATENTE NACIONAL n.º 119434	Data: 2024.05.13

Informa-se, que o pedido de Patente de Invenção em epígrafe irá ser objeto de publicação no Boletim da Propriedade Industrial n.º 209/2025 que será editado em 2025.10.29, nos termos do artigo 69.º do Código da Propriedade Industrial.

Mais se informa que, após essa publicação, qualquer pessoa que se sinta prejudicada poderá apresentar reclamação no prazo de dois meses a contar da data de publicação do referido Boletim.

Com os melhores cumprimentos,

Gisela Alexandre Fernandes
Técnico(a) Superior

MD128.05
Campo das Cebolas - 1149-035 Lisboa, Portugal
Tel. : +351 21 881 81 00 | Fax : +351 21 887 87 17
Linha de Atendimento INPI: +351 21 881 81 88 | E-mail: servico.publico@inpi.pt
Website: https://inpi.justica.gov.pt

7. REFERENCES

Abu-Qdais, H., & Al-Widyan, M. I. (2016). Evaluating composting and co-composting kinetics of various agro-industrial wastes. *International Journal of Recycling of Organic Waste in Agriculture*, 5(3), 273–280. https://doi.org/10.1007/s40093-016-0137-3

Abu-Thabit, N. Y., Judeh, A. A., Hakeem, A. S., Ul-Hamid, A., Umar, Y., & Ahmad, A. (2020). Isolation and characterization of microcrystalline cellulose from date seeds (*Phoenix dactylifera* L.). *International Journal of Biological Macromolecules*, 155, 730–739. https://doi.org/10.1016/j.ijbiomac.2020.03.255

AlGhamdi, K. M., Kumar, A., & Moussa, N. A. (2012). Low-level laser therapy: A useful technique for enhancing the proliferation of various cultured cells. *Lasers in Medical Science*, 27(1), 237–249. https://doi.org/10.1007/s10103-011-0885-2

Almeida, A., Neto, P., Pereira, I., Ribeiro, A., & Pilão, R. (2019). Effect of temperature on the gasification of olive bagasse particles. *Journal of the Energy Institute*, 92(1), 153–160. https://doi.org/10.1016/j.joei.2017.10.012

Almeida, A. P. C., Saraiva, J. N., Cavaco, G., Portela, R. P., Leal, C. R., Sobral, R. G., & Almeida, P. L. (2022). Crosslinked bacterial cellulose hydrogels for biomedical application. *European Polymer Journal*, 177, 111438. https://doi.org/10.1016/j.eurpolymj.2022.111438

Artem Petrosian. (2021). Production of bacterial cellulose from kombucha SCOBY: optimization of the bioprocess and industrial application. Master Dissertation in Biotechnological Engineering, Instituto Politécnico de Bragança.

Augimeri, R. V., & Strap, J. L. (2015). The phytohormone ethylene enhances cellulose production, regulates CRP/FNRKx transcription and causes differential gene expression within the bacterial cellulose synthesis operon of *Komagataeibacter* (*Gluconacetobacter*) *xylinus* ATCC 53582. *Frontiers in Microbiology*, 6, 169692. https://doi.org/10.3389/fmicb.2015.01459

Aslan, S., & Şirazi, M. (2020). Adsorption of Sulfonamide Antibiotic onto Activated Carbon Prepared from an Agro-industrial By-Product as Low-Cost Adsorbent: Equilibrium, Thermodynamic, and Kinetic Studies. *Water, Air, and Soil Pollution*, 231(5). https://doi.org/10.1007/s11270-020-04576-0

Avcioglu, N. H. (2022). Bacterial cellulose: recent progress in production and industrial applications. *World Journal of Microbiology and Biotechnology*, 38(5). https://doi.org/10.1007/s11274-022-03271-y

Berbel, J., & Posadillo, A. (2018). Review and analysis of alternatives for the valorisation of agro-industrial olive oil by-products. *Sustainability*, *10*(1), 237. https://doi.org/10.3390/su10010237

Bhat, R., W. N. Goh, Ahmad Rosma, Bhupinder Kaur, A. Fazilah, & Alias Abd Karim. (2012). Fermentation of black tea broth (Kombucha): I. Effects of sucrose concentration and fermentation time on the yield of microbial cellulose. *International Food Research Journal*, 19(1), 109-117.

Bohli, T., Ouederni, A., Fiol, N., & Villaescusa, I. (2015). Evaluation of an activated carbon from olive stones used as an adsorbent for heavy metal removal from aqueous phases. *Comptes Rendus Chimie*, 18(1), 88–99. https://doi.org/10.1016/j.crci.2014.05.009

Brown, R. M. (1996). The Biosynthesis of Cellulose. *Journal of Macromolecular Science, Part A*, *33*(10), 1345–1373. https://doi.org/10.1080/10601329608014912

Cabañas-Romero, L. V., Valls, C., Valenzuela, S. V., Roncero, M. B., Pastor, F. I. J., Diaz, P., & Martínez, J. (2020). Bacterial Cellulose–Chitosan Paper with Antimicrobial and Antioxidant Activities. *Biomacromolecules*, 21(4), 1568–1577. https://doi.org/10.1021/acs.biomac.0c00127

Campano, C., Balea, A., Blanco, A., & Negro, C. (2016). Enhancement of the fermentation process and properties of bacterial cellulose: a review. *Cellulose*, 23(1), 57–91. https://doi.org/10.1007/s10570-015-0802-0

Casadey, R., Challier, C., Altamirano, M., Spesia, M. B., & Criado, S. (2021). Antioxidant and antimicrobial properties of tyrosol and derivative compounds in the presence of vitamin B2. Assays of synergistic antioxidant effect with commercial food additives. *Food Chemistry*, 335, 127576. https://doi.org/10.1016/j.foodchem.2020.127576

Contreras, M. del M., Romero, I., Moya, M., & Castro, E. (2020). Olive-derived biomass as a renewable source of value-added products. *Process Biochemistry*, 97, 43–56. https://doi.org/10.1016/j.procbio.2020.06.013

Crugeira, P. J. L., Almeida, H. H. S., Marcet, I., Rendueles, M., Pires, M. G., Rafael, H. M., Rodrigues, A. I. G., Santamaria-Echart, A., & Barreiro, M. F. (2023). Biosynthesis of antioxidant xanthan gum by Xanthomonas campestris using substrates added with moist olive pomace. *Food and Bioproducts Processing*, 141, 210–218. https://doi.org/10.1016/j.fbp.2023.08.008

Crugeira, P. J. L., Pires Santos, G. M., de Oliveira, S. C. P. S., Sampaio, F. J. P., Fagnani, S. R. C. A., Sampaio, I. C. F., de Souza Ferreira, E., Chinalia, F. A., Pinheiro, A. L. B., & de

Almeida, P. F. (2019). Effects of photostimulation on the catabolic process of xenobiotics. *Journal of Photochemistry and Photobiology B: Biology*, 191, 38–43. https://doi.org/10.1016/j.jphotobiol.2018.12.004

Crugeira, P. J. L., Pires-Santos, G. M., de Oliveira, S. C. P. S., Sampaio, F. J. P., Correia, N. A., Fagnani, S. R. C. de A., Chinalia, F. A., de Almeida, P. F., & Pinheiro, A. L. B. (2018a). Photobiological effect of Laser or LED light in a thermophilic microbial consortium. *Journal of Photochemistry and Photobiology B: Biology*, 181, 115–121. https://doi.org/10.1016/j.jphotobiol.2018.03.006

Devanthi, P. V. P., Kho, K., Nurdiansyah, R., Briot, A., Taherzadeh, M. J., & Aslanzadeh, S. (2021). Do kombucha symbiotic cultures of bacteria and yeast affect bacterial cellulose yield in molasses? *Journal of Fungi*, *7*(9). https://doi.org/10.3390/jof7090705

Devanthi, P. V. P., Pratama, F., Kho, K., Taherzadeh, M. J., & Aslanzadeh, S. (2022). The Effect of *Dekkera bruxellensis* Concentration and Inoculation Time on Biochemical Changes and Cellulose Biosynthesis by *Komagataeibacter intermedius*. *Journal of Fungi*, *8*(11). https://doi.org/10.3390/jof8111206

Dima, S. O., Panaitescu, D. M., Orban, C., Ghiurea, M., Doncea, S. M., Fierascu, R. C., Nistor, C. L., Alexandrescu, E., Nicolae, C. A., Trica, B., Moraru, A., & Oancea, F. (2017). Bacterial nanocellulose from side-streams of kombucha beverages production: Preparation and physical-chemical properties. *Polymers*, *9*(8). https://doi.org/10.3390/polym9080374

Dochia, M., Sirghie, C., Kozłowski, R. M., & Roskwitalski, Z. (2012). Cotton fibres. In *Handbook of Natural Fibre,* 11–23. Elsevier. https://doi.org/10.1533/9780857095503.1.9

Fang, D. D. (2018). Cotton Fiber: Physics, Chemistry and Biology. In *Cotton Fiber: Physics, Chemistry and Biology*. Springer International Publishing. https://doi.org/10.1007/978-3-030-00871-0

Fernández, J., Morena, A. G., Valenzuela, S. V., Pastor, F. I. J., Díaz, P., & Martínez, J. (2019). Microbial Cellulose from a Komagataeibacter intermedius Strain Isolated from Commercial Wine Vinegar. *Journal of Polymers and the Environment*, *27*(5), 956–967. https://doi.org/10.1007/s10924-019-01403-4

alrdi, S., Hoffmann, T. G., Schmitz, F. R. W., Bertoli, S. L., Khayrullin, M., Neverova, O., Ponomarev, E., Goncharov, A., Kulmakova, N., Dotsenko, E., Khryuchkina, E., Shariati, M. A., & De Souza, C. K. (2021). Comprehensive study of Light-Emitting Diodes (LEDs) and Ultraviolet-LED lights application in food quality and safety. *Journal of Pure and Applied*

Microbiology, 15(3), 1125–1135. Journal of Pure and Applied Microbiology. https://doi.org/10.22207/JPAM.15.3.54

Gayathri, G. (2020). Studies on Bacterial Cellulose Production Using Industrial Wastewater (Doctoral dissertation, National Institute of Technology Karnataka, Surathkal).

Gomes, F. P., Silva, N. H. C. S., Trovatti, E., Serafim, L. S., Duarte, M. F., Silvestre, A. J. D., Neto, C. P., & Freire, C. S. R. (2013). Production of bacterial cellulose by *Gluconacetobacter sacchari* using dry olive mill residue. *Biomass and Bioenergy*, *55*, 205–211. https://doi.org/10.1016/j.biombioe.2013.02.004

Guindon, S., Dufayard, J.-F., Lefort, V., Anisimova, M., Hordijk, W., & Gascuel, O. (2010). New Algorithms and Methods to Estimate Maximum-Likelihood Phylogenies: Assessing the Performance of PhyML 3.0. *Systematic Biology*, *59*(3), 307–321. https://doi.org/10.1093/sysbio/syq010

Haydari, I., Lissaneddine, A., Aziz, K., Ouazzani, N., Mandi, L., El Ghadraoui, A., & Aziz, F. (2022). Optimization of preparation conditions of a novel low-cost natural bio-sorbent from olive pomace and column adsorption processes on the removal of phenolic compounds from olive oil mill wastewater. *Environmental Science and Pollution Research*, *29*(53), 80044–80061. https://doi.org/10.1007/s11356-022-20577-4

Hernández-Arriaga, A. M., del Cerro, C., Urbina, L., Eceiza, A., Corcuera, M. A., Retegi, A., & Auxiliadora Prieto, M. (2019). Genome sequence and characterization of the bcs clusters for the production of nanocellulose from the low pH resistant strain *Komagataeibacter medellinensis* ID13488. *Microbial Biotechnology*, *12*(4), 620–632. https://doi.org/10.1111/1751-7915.13376

Hsu, C. Y., Lin, S. C., Wu, Y. H., Hu, C. Y., Chen, Y. T., & Chen, Y. C. (2022). The Antimicrobial Effects of Bacterial Cellulose Produced by *Komagataeibacter intermedius* in Promoting Wound Healing in Diabetic Mice. *International Journal of Molecular Sciences*, *23*(10). https://doi.org/10.3390/ijms23105456

Huerta-Cepas, J., Serra, F., & Bork, P. (2016). ETE 3: Reconstruction, Analysis, and Visualization of Phylogenomic Data. *Molecular Biology and Evolution*, *33*(6), 1635–1638. https://doi.org/10.1093/molbev/msw046

Hussain, Z., Sajjad, W., Khan, T., & Wahid, F. (2019). Production of bacterial cellulose from industrial wastes: a review. *Cellulose*, 26(5), 2895–2911. https://doi.org/10.1007/s10570-019-02307-1

Jayabalan, R., Malbaša, R. V., Lončar, E. S., Vitas, J. S., & Sathishkumar, M. (2014). A review on kombucha tea-microbiology, composition, fermentation, beneficial effects, toxicity, and tea fungus. *Comprehensive Reviews in Food Science and Food Safety*, 13(4), 538–550). https://doi.org/10.1111/1541-4337.12073

Jing Wang, Javad Tavakolib, & Youhong Tangb. (2019). Bacterial cellulose production, properties and applications with different culture methods – A review. *Carbohydrate Polymers*, 219, 63–76.

Karu, T. (1999). Primary and secondary mechanisms of action of visible to near-IR radiation on cells. *Journal of Photochemistry and Photobiology B: Biology*, *49*(1), 1–17. https://doi.org/10.1016/S1011-1344(98)00219-X

Karu, T. I., Pyatibrat, L. V., & Kalendo, G. S. (2004). Photobiological modulation of cell attachment via cytochrome c oxidase. *Photochemical & Photobiological Sciences*, *3*(2), 211–216. https://doi.org/10.1039/b306126d

Kazan, A., Celiktas, M. S., Sargin, S., & Yesil-Celiktas, O. (2015). Bio-based fractions by hydrothermal treatment of olive pomace: Process optimization and evaluation. *Energy Conversion and Management*, *103*, 366–373. https://doi.org/10.1016/j.enconman.2015.06.084

Keshk, S. M. A. S., & Sameshima, K. (2005). Evaluation of different carbon sources for bacterial cellulose production. *African Journal of Biotechnology*, *4*(6), 478-482.

Khan, S. B., & Kamal, T. (Eds.). (2021). *Bacterial Cellulose: Synthesis, Production, and Applications*. CRC Press.

Khwaldia, K., Attour, N., Matthes, J., Beck, L., & Schmid, M. (2022). Olive byproducts and their bioactive compounds as a valuable source for food packaging applications. *Comprehensive Reviews in Food Science and Food Safety*, *21*(2), 1218–1253. https://doi.org/10.1111/1541-4337.12882

Klemm, D., Heublein, B., Fink, H. P., & Bohn, A. (2005). Cellulose: Fascinating biopolymer and sustainable raw material. *Angewandte Chemie - International Edition*, 44(22), 3358–3393. https://doi.org/10.1002/anie.200460587

Kongruang, S. (2008). Bacterial cellulose production by Acetobacter xylinum strains from agricultural waste products. In *Biotechnology for Fuels and Chemicals: Proceedings of the Twenty-Ninth Symposium on Biotechnology for Fuels and Chemicals Held April 29–May 2, 2007, in Denver, Colorado* (763-774). https://doi.org/10.1007/s12010-007-8119-6

Kopka, B., Magerl, K., Savitsky, A., Davari, M. D., Röllen, K., Bocola, M., Dick, B., Schwaneberg, U., Jaeger, K.-E., & Krauss, U. (2017). Electron transfer pathways in a light, oxygen, voltage (LOV) protein devoid of the photoactive cysteine. *Scientific Reports*, *7*(1). https://doi.org/10.1038/s41598-017-13420-1

Krzysztof Jadczak, W. O.-S. (2023). Bacterial cellulose: Biopolymer with novel medical applications. *Journal of Biomaterials Applications*, 38(1), 51–63.

Kumbhar, J. V., Rajwade, J. M., & Paknikar, K. M. (2015). Fruit peels support higher yield and superior quality bacterial cellulose production. *Applied Microbiology and Biotechnology*, *99*(16), 6677–6691. https://doi.org/10.1007/s00253-015-6644-8

Lee, K. Y., Buldum, G., Mantalaris, A., & Bismarc, A. (2014). More than meets the eye in bacterial cellulose: Biosynthesis, bioprocessing, and applications in advanced fiber composites. *Macromolecular Bioscience*, *14*(1), 10–32. https://doi.org/10.1002/mabi.201300298

Leite, L. (2021). Isolamento e identificação molecular de bactérias e leveduras de SCOBY e sua aplicação na produção de celulose bacteriana. *Relatório de Estágio de Licenciatura em Biologia e Biotecnologia*, Instituto Politécnico de Bragança.

Leite, P., Salgado, J. M., Venâncio, A., Domínguez, J. M., & Belo, I. (2016). Ultrasounds pretreatment of olive pomace to improve xylanase and cellulase production by solid-state fermentation. *Bioresource Technology*, *214*, 737–746. https://doi.org/10.1016/j.biortech.2016.05.028

Lestari, P., Elfrida, N., Suryani, A., & Suryadi, Y. (2014). Study on the Production of Bacterial Cellulose from *Acetobacter xylinum* Using Agro-Waste. *Jordan Journal of Biological Sciences*, *7*(1), 75–80. https://doi.org/10.12816/0008218

Liang, S. (2023). Advances in drug delivery applications of modified bacterial cellulose-based materials. *Frontiers in Bioengineering and Biotechnology*, *11*. https://doi.org/10.3389/fbioe.2023.1252706

Lin, S. P., Loira Calvar, I., Catchmark, J. M., Liu, J. R., Demirci, A., & Cheng, K. C. (2013). Biosynthesis, production and applications of bacterial cellulose. *Cellulose*, 20(5), 2191–2219. https://doi.org/10.1007/s10570-013-9994-3

Lin, S.-P., Huang, Y.-H., Hsu, K.-D., Lai, Y.-J., Chen, Y.-K., & Cheng, K.-C. (2016). Isolation and identification of cellulose-producing strain *Komagataeibacter intermedius* from fermented fruit juice. *Carbohydrate Polymers*, *151*, 827–833. https://doi.org/10.1016/j.carbpol.2016.06.032

Lobiuc, A., Pavăl, N. E., Mangalagiu, I. I., Gheorghiță, R., Teliban, G. C., Amăriucăi-Mantu, D., & Stoleru, V. (2023). Future Antimicrobials: Natural and Functionalized Phenolics. *Molecules.* 28(3). MDPI. https://doi.org/10.3390/molecules28031114

Madureira, J., Melgar, B., Santos-Buelga, C., Margaça, F. M., Ferreira, I. C., Barros, L., & Cabo Verde, S. (2021). Phenolic compounds from irradiated olive wastes: Optimization of the heat-assisted extraction using response surface methodology. *Chemosensors*, *9*(8), 231. https://doi.org/10.3390/chemosensors9080231

Matsumura, K., & Rajan, R. (2021). Oxidized polysaccharides as green and sustainable biomaterials. *Current Organic Chemistry*, *25*(13), 1483-1496. https://doi.org/10.2174/1385272825666210428140052

Mensah, A., Chen, Y., Christopher, N., & Wei, Q. (2022). Membrane Technological Pathways and Inherent Structure of Bacterial Cellulose Composites for Drug Delivery. *Bioengineering* 9(1). https://doi.org/10.3390/bioengineering9010003

Moniri, M., Moghaddam, A. B., Azizi, S., Rahim, R. A., Ariff, A. Bin, Saad, W. Z., Navaderi, M., & Mohamad, R. (2017). Production and status of bacterial cellulose in biomedical engineering. *Nanomaterials*, 7(9). https://doi.org/10.3390/nano7090257

Moyes, R. B., Reynolds, J., & Breakwell, D. P. (2009). Differential staining of bacteria: Gram stain. *Current Protocols in Microbiology*,15. https://doi.org/10.1002/9780471729259.mca03cs15

Naomi, R., Idrus, R. B. H., & Fauzi, M. B. (2020). Plant-vs. Bacterial-derived cellulose for wound healing: A review. In *International Journal of Environmental Research and Public Health,* 17 (18), 1–25. https://doi.org/10.3390/ijerph17186803

Nizer, W. S. da C., Inkovskiy, V., & Overhage, J. (2020). Surviving reactive chlorine stress: Responses of gram-negative bacteria to hypochlorous acid. *Microorganisms,* 8(8), 1–27. https://doi.org/10.3390/microorganisms8081220

madu, M. A., Pimentel, F. B., Costa, A. S. G., Alves, R. C., & Oliveira, M. B. P. P. (2016). Olive by-products for functional and food applications: Challenging opportunities to face environmental constraints. *Innovative Food Science and Emerging Technologies* 35, 139–148. https://doi.org/10.1016/j.ifset.2016.04.016

Okiyama, A., Shirae, H., Kano, H., & Yamanaka, S. (1992). Bacterial cellulose I. Two-stage fermentation process for cellulose production by *Acetobacter aceti*. *Topics in Catalysis*, *6*(5), 471–477. https://doi.org/10.1016/S0268-005X(09)80032-5

Payen, A. (1838). Mémoire sur la composition du tissu propre des plantes et du ligneux. *Comptes* rendus, 7(lu 17 décembre 1838), 1052-1056.

Passarella, S., & Karu, T. (2014). Absorption of monochromatic and narrow band radiation in the visible and near IR by both mitochondrial and non-mitochondrial photoacceptors results in photobiomodulation. *Journal of Photochemistry and Photobiology B: Biology*, *140*, 344-358. https://doi.org/10.1016/j.jphotobiol.2014.07.021

Pinheiro, A. L. B., de Almeida, P. F., Sampaio, I. C. F., Crugeira, P. J. L., dos Santos, J. N., Matos, J. B. T. L., Soares, L. G. P., Moraga Amador, D. A., & Silveira, L. (2020). Effects of photo-stimulation with laser or LED on the composition of Xanthan gum produced in media containing distilled water or dialyzed or not produced water by means of Raman spectroscopy. *Journal of Photochemistry and Photobiology B: Biology*, *213*. https://doi.org/10.1016/j.jphotobiol.2020.112057

Popa, L., Ghica, M. V., Tudoroiu, E. E., Ionescu, D. G., & Dinu-Pîrvu, C. E. (2022). Bacterial Cellulose—A Remarkable Polymer as a Source for Biomaterials Tailoring. *Materials*, 15, (3). MDPI. https://doi.org/10.3390/ma15031054

Poulin, M. B., & Kuperman, L. L. (2021). Regulation of Biofilm Exopolysaccharide Production by Cyclic Di-Guanosine Monophosphate. *Frontiers in Microbiology*, *12*. https://doi.org/10.3389/fmicb.2021.730980

Prabhakaran, P., Ashraf, M. A., & Aqma, W. S. (2016). Microbial stress response to heavy metals in the environment. *RSC Advances*. 6(111), 109862–109877. https://doi.org/10.1039/c6ra10966g

Przygrodzka, K., Charęza, M., Banaszek, A., Zielińska, B., Ekiert, E., & Drozd, R. (2022). Bacterial Cellulose Production by *Komagateibacter xylinus* with the Use of Enzyme-Degraded Oligo- and Polysaccharides as the Substrates. *Applied Sciences (Switzerland*), 12(24). https://doi.org/10.3390/app122412673

Raghavendran, V., Asare, E., & Roy, I. (2020). Bacterial cellulose: Biosynthesis, production, and applications. *Advances in Microbial Physiology* 77, 89–138. https://doi.org/10.1016/bs.ampbs.2020.07.002

Ramana, K. V, Tomar, A., & Singh, L. (2000). Ramana, K. V., Tomar, A., & Singh, L. (2000). Effect of various carbon and nitrogen sources on cellulose synthesis by Acetobacter xylinum. *World Journal of Microbiology and Biotechnology*, *16*, 245-248.

Reis, D. T., Pereira, A. K. D. S., Scheidt, G. N., & Pereira, D. H. (2019). Plant and bacterial cellulose: Production, chemical structure, derivatives and applications. *Orbital* 11(5), 321–

329. Universidade Federal de Mato Grosso do Sul, Departamento de Química. https://doi.org/10.17807/orbital.v11i5.1349

Ryngajłło, M., Jędrzejczak-Krzepkowska, M., Kubiak, K., Ludwicka, K., & Bielecki, S. (2020). Towards control of cellulose biosynthesis by *Komagataeibacter* using systems-level and strain engineering strategies: current progress and perspectives. *Applied Microbiology and Biotechnology*, 10*4*, 6565–6585. https://doi.org/10.1007/s00253-020-10671-3/Published

Sagdic-Oztan, C., Koschella, A., Heinze, T., Karaguler, N. G., & Tuter, M. (2023). Preparation of bacterial cellulose using enzymatic hydrolysate of olive pomace as carbon source. *BioResources*, *18*(2), 4168–4181. https://doi.org/10.15376/biores.18.2.4168-4181

Santoso, S. P., Chou, C.-C., Lin, S.-P., Soetaredjo, F. E., Ismadji, S., Hsieh, C.-W., & Cheng, K. C. (2020). Enhanced production of bacterial cellulose by *Komactobacter intermedius* using statistical modeling. *Cellulose*, *27*(5), 2497–2509. https://doi.org/10.1007/s10570-019-02961-5

Sar, T., & Yesilcimen Akbas, M. (2022). Potential use of olive oil mill wastewater for bacterial cellulose production. *Bioengineered*, *13*(3), 7659-7669. https://doi.org/10.1080/21655979.2022.2050492

Seval Dağbağlı, Y. G. (2017). Exopolysaccharide production of acetic acid bacteria. In *Acetic Acid Bacteria* (pp. 120-141). CRC Press.. https://doi.org/10.1201/9781315153490

Shalaby, S., & Horwitz, B. A. (2015). Plant phenolic compounds and oxidative stress: integrated signals in fungal–plant interactions. *Current genetics*, *61*, 347-357. https://doi.org/10.1007/s00294-014-0458-6

Tsouko, E., Kourmentza, C., Ladakis, D., Kopsahelis, N., Mandala, I., Papanikolaou, S., Paloukis, F., Alves, V., & Koutinas, A. (2015). Bacterial Cellulose Production from Industrial Waste and by-Product Streams. *International Journal of Molecular Sciences*, *16*(12), 14832–14849. https://doi.org/10.3390/ijms160714832

Urbina, L., Corcuera, M. Á., Gabilondo, N., Eceiza, A., & Retegi, A. (2021). A review of bacterial cellulose: sustainable production from agricultural waste and applications in various fields. *Cellulose* 28(13), 8229–8253). https://doi.org/10.1007/s10570-021-04020-4

Vadanan, S. V. (2020). Bacterial cellulose: from culturing to the development of functional materials, Nanyang Technological University. https://doi.org/10.32657/10356/143357

Velásquez-Riaño, M., & Bojacá, V. (2017). Production of bacterial cellulose from alternative low-cost substrates. *Cellulose*, *24*, 2677-2698. https://doi.org/10.1007/s10570-017-1309-7

Wang, S.-S., Han, Y.-H., Chen, J.-L., Zhang, D.-C., Shi, X.-X., Ye, Y.-X., Chen, D.-L., & Li, M. (2018). Insights into Bacterial Cellulose Biosynthesis from Different Carbon Sources and the Associated Biochemical Transformation Pathways in *Komagataeibacter* sp. W1. *Polymers*, *10*(9), 963. https://doi.org/10.3390/polym10090963

Wook Hwang, J., Kook Yang, Y., Kwan Hwang, J., Ryang Pyun, Y., & Sam Kim, Y. (1999). Effects of pH and dissolved oxygen on cellulose production by Acetobacter xylinum BRC5 in agitated culture. *Journal of Bioscience and Bioengineering*, *88*(2), 183-188. https://doi.org/10.1016/S1389-1723(99)80199-6

Yim, S. M., Song, J. E., & Kim, H. R. (2017). Production and characterization of bacterial cellulose fabrics by nitrogen sources of tea and carbon sources of sugar. *Process Biochemistry*, *59*, 26–36. https://doi.org/10.1016/j.procbio.2016.07.001